AD_____

Award Number: DAMD17-97-1-7207

TITLE: Template Based Design of Anti-Metastatic Drugs from the Active Conformation of Laminin Peptide II

PRINCIPAL INVESTIGATOR: Jean R. Starkey, DVM, Ph.D.

CONTRACTING ORGANIZATION: Montana State University
Bozeman, Montana 59717-2470

REPORT DATE: January 2000

TYPE OF REPORT: Annual

PREPARED FOR: U.S. Army Medical Research and Materiel Command
Fort Detrick, Maryland 21702-5012

REPORT DOCUMENTATION PAGE

Form Approved
OMB No. 074-0188

1. AGENCY USE ONLY (Leave blank)	2. REPORT DATE	3. REPORT TYPE AND DATES COVERED
	January 2000	Annual (1 Jan 99 - 31 Dec 99)

4. TITLE AND SUBTITLE
Template Based Design of Anti-Metastatic Drugs from the Active Conformation of Laminin Peptide II

5. FUNDING NUMBERS
DAMD17-97-1-7207

6. AUTHOR(S)
Jean R. Starkey, DVM, Ph.D.

7. PERFORMING ORGANIZATION NAME(S) AND ADDRESS(ES)
Montana State University
Bozeman, Montana 59717-2470

E-MAIL:
zmb7004@msu.oscs.montana.edu

8. PERFORMING ORGANIZATION REPORT NUMBER

9. SPONSORING / MONITORING AGENCY NAME(S) AND ADDRESS(ES)
U.S. Army Medical Research and Materiel Command
Fort Detrick, Maryland 21702-5012

10. SPONSORING / MONITORING AGENCY REPORT NUMBER

11. SUPPLEMENTARY NOTES

12a. DISTRIBUTION / AVAILABILITY STATEMENT
Approved for public release; distribution unlimited

12b. DISTRIBUTION CODE

13. ABSTRACT ***(Maximum 200 Words)***

Additional work has been conducted to elucidate the structure of the peptide 11 binding pocket in the 67 kDa LBP. Limited proteolysis experiments on the rLBP indicated that all the regions, identified last year by phage display as interacting with peptide 11, were surface exposed on the folded protein. We found that the recombinant protein exhibited partial aggregation driven by disulfide bond formation at the very high concentrations needed for NMR spectroscopy, and we have created mutant rLBP lacking Cys residues to alleviate this problem. The candidate 16 mimetic has been synthesized, as well as a useful structural relative which can be produced in many chiral variants for determining the optimal geometry for anti-invasive activity. We found that ER +ve tumor cells shed LBP in amounts proportional to their invasive abilities. 17β estradiol promoted LBP shedding, and addition of exogenous shed or rLBP promoted invasion by ER +ve breast and ovarian cancer cells. LBP shedding may turn out to be a new therapeutic target. The LBP protein was found to have sulfhydryl oxidase activity, a finding potentially related to the optimal activity of peptide 11 dimer and the loss of activity in the Ser for Cys peptide 11 analog.

14. SUBJECT TERMS
Breast Cancer, invasion, metastasis, laminin binding protein, Peptide 11, NMR, mimetic

15. NUMBER OF PAGES
40

16. PRICE CODE

17. SECURITY CLASSIFICATION OF REPORT	18. SECURITY CLASSIFICATION OF THIS PAGE	19. SECURITY CLASSIFICATION OF ABSTRACT	20. LIMITATION OF ABSTRACT
Unclassified	Unclassified	Unclassified	Unlimited

FOREWORD

Opinions, interpretations, conclusions and recommendations are those of the author and are not necessarily endorsed by the U.S. Army.

___ Where copyrighted material is quoted, permission has been obtained to use such material.

___ Where material from documents designated for limited distribution is quoted, permission has been obtained to use the material.

___ Citations of commercial organizations and trade names in this report do not constitute an official Department of Army endorsement or approval of the products or services of these organizations.

JMS
X In conducting research using animals, the investigator(s) adhered to the "Guide for the Care and Use of Laboratory Animals," prepared by the Committee on Care and use of Laboratory Animals of the Institute of Laboratory Resources, national Research Council (NIH Publication No. 86-23, Revised 1985).

JMS
X For the protection of human subjects, the investigator(s) adhered to policies of applicable Federal Law 45 CFR 46.

JMS
X In conducting research utilizing recombinant DNA technology, the investigator(s) adhered to current guidelines promulgated by the National Institutes of Health.

JMS
X In the conduct of research utilizing recombinant DNA, the investigator(s) adhered to the NIH Guidelines for Research Involving Recombinant DNA Molecules.

N/A In the conduct of research involving hazardous organisms, the investigator(s) adhered to the CDC-NIH Guide for Biosafety in Microbiological and Biomedical Laboratories.

Donald Stathis, May 2-2000

PI - Signature Date

Table of Contents

Cover.....01

SF 298.....02

Foreword.....03

Table of Contents.....04

Introduction.....05

Body.....06

Key Research Accomplishments.....34

Reportable Outcomes.....35

Conclusions.....36

References.....38

Appendices.....None

Introduction

Many clinical studies on breast cancer and other solid tumors show strong positive correlations of high expression of the 67 kDa laminin binding protein (LBP) with poor prognosis [1,2,3,4,5,6,7,8,9,10,11]. The 67 kDa LBP has been shown to be a legitimate target for cancer therapy by the demonstration that reduction of tumor cell expression of the 67 kDa LBP, brought about by anti-sense or antibody approaches does inhibit tumor metastasis in mice [12,13,14]. However, current limitations with gene and antibody therapies restrict the use of these approaches for long term clinical applications. Our approach is to use the active conformation of the matrix ligand for the 67 kDa LBP as a template for the design of orally compatible anti-metastatic drugs. This ligand has been identified as a nine amino acid sequence from laminin-1, CDPGYIGSR, and is known as peptide 11 [15,16]. The actual mimetics are designed to represent only the YIGSR region of bound peptide 11, because YIGSR is known to be the minimal active sequence [16] and synthesis of organic mimetics for longer sequences than this is daunting.

The ability of synthetic peptide 11 or YIGSR to block tumor cell invasion and metastasis depends on its ability to interfere with the interactions of the 67 kDa LBP with basement membrane laminin-1 [15,16]. The 67 kDa LBP (a dimer from the 37 kDa LBP gene product) derives from the S2 ribosomal class of proteins [17], a unique evolution having occurred in the C-terminal domain in parallel with the appearance of laminin and laminin-like molecules [17]. This C-terminal domain has been indicated by us and others as the matrix ligand binding domain [18,19,20,21]. The half-life of peptide 11 (and YIGSR) in the bloodstream is in the order of minutes, consistent with rapid proteolysis [22]. Therefore, in order to develop useful therapeutics, either the biological half-life of peptide 11 must be very significantly extended, or else it is essential to mimic the properties of peptide 11 using non-peptide compounds. The overall goal of this research project is to design accurate mimetics using template -based approaches, and to evaluate their anti-invasive and anti-metastatic activity. If we are successful in synthesizing mimetics with good anti-metastatic activity, this will provide a "proof of concept" for our structure -based design approach, and the best mimetics should be effective lead compounds suitable for going into combinatorial chemistry programs to provide the most effective derivatives.

There are three specific aims that should allow us to accomplish the goal of this research project:

Aim 1 In collaboration with Drs. V. Copié and E. A. Dratz, of the Chemistry and Biochemistry Department at MSU[1], to determine the relevant structural characteristics of the ligand binding domain of the LBP.

Aim 2 In collaboration with Dr. W. Todd Wipke, Professor of Chemistry and Biochemistry, UCSC[2], to undertake structure-based design of non-peptide mimetics for the active conformation of peptide 11 using INVENTON, an artificially intelligent computer program for the design of structural mimetic compounds.

Aim 3 In collaboration with Dr. J. Konopelski, UCSC, to synthesize the most promising structures derived by the INVENTON program, and to evaluate the activities of the new compounds in inhibiting tumor cell invasion *in vitro*, and metastasis in experimental animals.

[1] MSU = Montana State University
[2] UCSC = University of California, Santa Cruz

Body of Report

This is a highly collaborative project with contributions from five different laboratories and two different institutions. It follows that the "statement of work" is complex, and for convenience of the reader, we re-iterate it below.

STATEMENT OF WORK:

Technical Objective (aim) 1

Task 1: Months 1-15: Determine the LBP residues which interact with peptide 11.

Task 2: Months 1-18: Express the ligand binding domain of the LBP in *E. coli*, conduct multidimensional NMR experiments to determine structural information relevant to drug design.

Task 3: Months 1-15: Provide all relevant information from Tasks 1-2 of this proposal, along with the fully refined bound peptide 11 conformation **(derived from work carried out exclusively on our NIH award)**, to Dr. Wipke to improve the peptide 11 template used by INVENTON for the design of peptide mimics.

Technical Objective (aim) 2

Task 4: Months 6-18: Using the artificially intelligent program, INVENTON, design mimics of the LBP-bound conformation of peptide 11 (actually the YIGSR domain from this structure).

Task 5: Months 12-18: Integrate new information coming from tasks 1-3 into the drug design template used by INVENTON.

Task 6: Months 6-18: Evaluate the output structures from INVENTON for potential drug lead compounds. Synthesize the most approachable of these.

Task 7: Months 6-18: Work with Dr. Wipke's group in providing heuristic rules for determining the relative ease of synthesis for output structures from INVENTON.

Task 8: Months 12-22: Provide Dr. Starkey's group with mimetic compounds for limited preclinical tests.

Technical Objective (aim) 3

Task 9: Months 1-12: Test informative analogs of peptide 11 for anti-invasive and anti-metastatic activity.

Task 10: Months 12-24: Test mimetic compounds for 1) tissue culture toxicity, 2) anti-invasive activity and 3) anti-metastatic activity.

Progress on Technical Objective 1, task 1. (Bold = 2nd year activity)

Experimental Methods and Procedures

The methodology originally outlined in the grant application was restricted to mapping the contact residues in the LBP by using our photo-crosslinking biotinylated analog of peptide 11 [23]. The derivatized LBP and its cleavage fragments would be isolated using monovalent avidin matrices, and final analysis would be carried out using mass spectrometry sequencing techniques. The proposed methodology for isolating derivatized LBP and cleavage products relied on the use of one of the two commercially available monovalent avidin matrices. Unfortunately, both gave very poor yields and commercial anti-biotin antibodies were found to exhibit very low affinities. We, therefore, made our own rabbit antibodies for this work. Appropriate antibody specificity was sought using immunizing antigens consisting of biotin and biotinylated peptide 11 crosslinked to an irrelevant protein (KLH - keyhole limpet hemocyanin). After removal of KLH specific responses, we tested the antibodies by Western blot analysis. Good titers were found to biotinylated proteins and derivatized LBP. **The antibody still exhibited unwanted cross-reactions, and so was further purified over a peptide 11 column. The resultant product provided a highly specific reagent capable of isolating derivatized LBP from detergent extracts of tumor cell membranes. However, yields of derivatized LBP from whole cell membranes were still problematic, and we have moved to using rLBP for these experiments.**

Limited proteolysis experiments were carried out on isolated recombinant LBP using trypsin and elastase. Both proteases yielded useful sized fragments which were purified by HPLC and then sequenced. Interestingly, surface exposed (detectable early in the time course) cleavage sites were found in all regions which were predicted by our phage display mapping experiments to interact with peptide 11. The same cleavage, isolation and sequencing experiments will be carried out on photocrosslinked rLBP to determine the contact residues for peptide 11. Since we have excellent production of rLBP from our bacterial vectors, we can use regular amino acid sequencing approaches rather than the originally proposed mass spectrometry ones. This simplifies the work a great deal making it possible to complete the mapping of peptide 11 contact residues in rLBP within the time frame of this award.

Because of the initial difficulties with isolating sufficient derivatized LBP from tumor cell membranes, we carried out a series of experiments using phage display mapping to identify sequences within the LBP which interact with peptide 11. This alternative experimental approach cannot provide the detail to identify the actual contact residues, but, nonetheless, can provide very useful preliminary data identifying the interacting sequences. The J404 9-mer random phage display library [24] was used to identify sequences which bind to laminin-1 and elute with heparan sulfate or peptide 11. Laminin-1 derivatized plates were used for biopanning. Three consecutive rounds of low pH elutions were carried out, followed by three rounds of specific elutions; each consisting of a heparan sulfate elution followed by a peptide 11 (CDPGYIGSR) elution. The random sequence inserts were sequenced for phage populations eluted at low pH, by heparan sulfate and by peptide 11. The phage insert sequences were then compared to the sequence of the LBP looking for similarities which would identify regions of the LBP which could bind to peptide 11. Heparan sulfate elution was included as previous work has suggested that heparin mediated binding of the LBP to laminin-1 could occur in some cases [25,26]. **Scrambled peptide 11 (SRYDGGICP) and an irrelevant bioactive peptide derived from laminin-1 (APSTLEGRPSAY) were used in parallel experiments to elute phage from laminin-1. 40 phage were sequenced from the populations eluted by each of these control peptides. Only one sequence similar to the peptide 11**

eluted sequences was found amongst the scrambled peptide 11 eluted phage sequences, and none were found for the APSTLEGRPSAY eluted phage sequences. The results from these control peptides demonstrated specificity for the peptide 11 eluted phage sequences.

Assumptions

We anticipated that results from the phage display experiments would identify sequences within the LBP which contain the contact residues for peptide 11.

Results

Table 1. Sample mimotopes and putative heparin binding sequences obtained from phage specifically eluted from laminin-1 by peptide 11 or by heparin/heparan sulfate

Sequence homology[2] with:	Sequences from phage eluted by peptide 11[1]	Sequences eluted by heparin/heparan sulfate[1]
LBP$^{205-229}$	RDPEEIEKEEQAAAEKAVTKEEFQG GM**KAVR** **IQG**	RDPEEIEK EEQAAAEKAVTKEEFQG **DR**TAM**QVAA** **DRTA**MQVAA **VVSK**IS**EAG** GGS**VA**F**RAG**
LBP - Peptide G	IPCNNKGAHSVGLMWWMLAREVLRMR KP**WW**R**T**NTA (6) WHRT**MWWW**P (8) P**WWWM**TR**H**W[3]	IPCNNKGAHSVGLMWWMLAREVLRMR GPG**AWW**GS**A**
LBP - C-terminal DWS containing repeats	QPATEDWS **QN** **TD** **W**LGNL (3)	QPATEDWS None
Putative heparin binding sequences[4]	**H**AR**S**H**Y**PWY **KW**K**W**PD**R**P**K** SLE**HR**AF**R**N VPFYS**H**S**K**L G**K**LNLGGY**K** **K**MN**K**GVVNP	S**K**M**HR**NSWF A**K**IPAG**R**D**R** VPFYS**H**S**K**V **K**MN**K**GVVNP

[1] Residues contributing to the homology are shown in bold and underlined.
[2] Residues showing homology with the mimotopes are underlined.
[3] Previous sequence in reverse order.
[4] Positively charged residues are shown in bold.
[5] Number of multiple isolations are shown in parentheses.

Specifically eluted phage populations exhibited three classes of mimotopes for different regions in the cDNA derived amino acid sequence of the 67 kDa laminin binding protein (LBP). These regions were 1) a palindromic sequence known as peptide G, 2) a predicted helical domain corresponding to LBP residues 205-229, and 3) TEDWS -containing C-terminal repeats (Table 1). All elution conditions also yielded phage with putative heparin binding sequences (Table 1). We modeled the LBP$^{205-229}$ domain, which we

demonstrated by circular dichroism (CD) to have a helical secondary structure, and determined that this region likely possesses heparin binding characteristics located to one side of the helix, while the opposite side may contain a hydrophobic patch where peptide 11 could bind. Using Elisa plate assays, we demonstrated that peptide 11 and heparan sulfate both individually bound to synthetic $LBP^{205-229}$ peptide. We also demonstrated that synthetic PATEDWSA peptide could inhibit tumor cell adhesion to laminin-1. These data support the proposal that the 67 kDa LBP can bind the β-1 laminin chain at the peptide 11 region, and suggest that heparan sulfate is a likely alternate ligand for the binding interactions. Our results also confirm previous data [27] suggesting that the most C-terminal region of the LBP, which contains the TEDWS repeats, is involved in cell adhesion to laminin-1, and we specifically indicated the repeat sequence in that activity. **These results have been accepted for publication by J. Mol. Biol. The publication date is may 5, 2000, so reprints are not available yet to append to this report.**

As indicated earlier, limited proteolysis experiments, carried out on well folded samples of rLBP, demonstrated that all three regions indicated by the phage display experiments as interacting with peptide 11, were on the surface of the protein. This data strongly supports our interpretation of the phage display results.

Discussion and Recommendations

These experiments indicate that peptide 11 interacts with three different sequences domains in the 67 kDa LBP. The data also suggests that heparin/heparan sulfate is an alternate ligand for the 67 kDa LBP. As expected, the ligand binding domain of the LBP appears to be quite complex. Any structures which we develop for the active conformation of peptide 11, and for the ligand binding domain of the LBP, should be compatible with these data on peptide 11 interacting sequences. **The success of the limited proteolysis experiments indicates that we should be able to complete the goal of mapping peptide 11 contact residues in an expeditious manner.**

Progress on Technical Objective 1, task 2. (Bold =2nd year activity)

Experimental Methods and Procedures

Expression of the ligand binding domain of the LBP in ***E. coli***: This work is being carried out in collaboration with Dr. Valérie Copié at Montana State University. The first step in conducting the NMR structural studies of the ligand binding domain of the LBP is to express this domain in bacteria. This will allow for heavy isotope labeling of the domain at reasonable cost. The coding region for the full length expression product was obtained from our mammalian vector and cloned into the pTrcHis B prokaryotic expression vector (Invitrogen). Top 10 *E. coli* cells (Invitrogen) were successfully transformed, and they produced a protein of the correct molecular weight which stained positively with our anti-LBP antibody in a Western blot. However, the Trp promoter in this vector is not particularly efficient, and only modest yields of the LBP were obtained.

A second vector was then tried. This is the pET-30 vector from Novagen which utilizes the more efficient T7 promoter system. This time we used CD41 *E. coli* cells which have been successfully used in our hands to produce isotopically labeled peptides. On induction with IPTG (Isopropyl-β-D-thiogalactopyranoside), large quantities of the expressed LBP were obtained (Figure 1), and the same was the case for the C135 LBP ligand binding domain. We utilized the N-terminal poly-His tag for isolation

of the expressed recombinant protein by Ni affinity (Figure 2) The pET-30 vector contains two N-terminal protease cleavage sites for removing the poly-His tag. Closest to the expressed protein sequence is an enterokinase site. We abandoned this site when we could not achieve cleavage efficiencies greater than 50%. The more distant thrombin cleavage site worked very well with close to 100% efficiency (Figure 3). Biotinylated thrombin is used for the cleavage, and it is easily removed from the expressed protein preparation over a streptavidin column. Free poly-His sequence is removed by a second pass over the Ni column. It is clear that the pET-30 vector system would work well for our needs. A final refinement, now being attempted, is to utilize a modification of this vector, pET-15b which does not contain an enterokinase cleavage site, and which has the thrombin cleavage site immediately N-terminal to the expressed protein sequence. This vector would provide expressed protein without any additional irrelevant sequence from the vector construct. **Following more work to compare the two vectors, the pET-15b vector was chosen for this project as it produced large quantities of recombinant heavy isotope lablelled protein, and because preparation of the purified LBP was simpler (see above).**

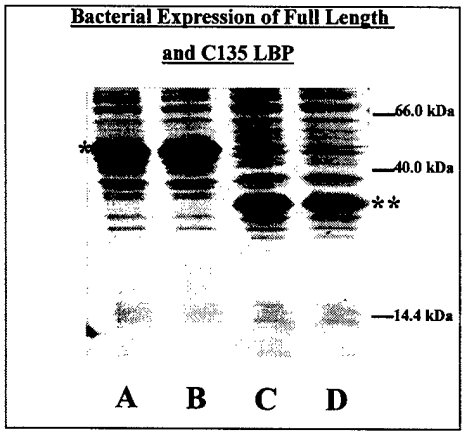

Figure 1. Whole bacterial cell lysates resolved on Coomassie Blue stained SDS-PAGE gels. Asterisks indicate the positions of the recombinant LBP products.

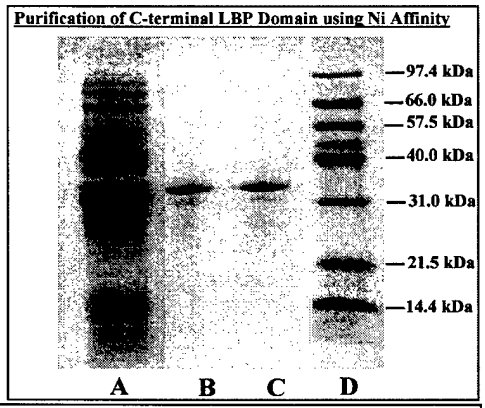

Figure 2. Purification of C135 LBP expression product using Ni affinity. SDS-PAGE gel stained with Coomassie Blue. Lane A = whole cell lysate, lanes B and C = imidazole eluate from the Ni column, lane D = molecular weight markers.

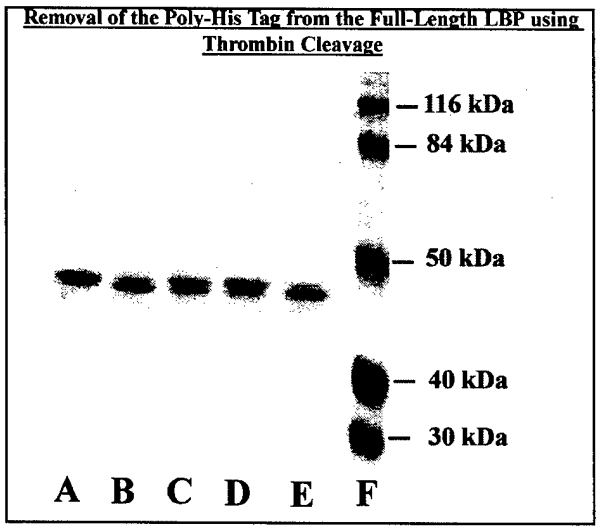

Figure 3. Full length LBP bacterial product resolved on a Coomassie Blue stained SDS-PAGE gel. Lane A = uncut product, lanes B-D = product partially cleaved by thrombin, lane E = fully cleaved product, lane F = molecular weight standards.

The molecular weight of the isolated expressed C135 ligand binding domain was checked by time of flight MALDI (matrix assisted laser desorption) mass spectrometry, and the success of refolding the domain by circular dichroism (CD) spectroscopy.

The recombinant C135 domain labelled well with ^{15}N, a prerequisite for NMR studies. However, while this domain remained well folded at low and medium concentrations, at the high concentrations needed for NMR structure determination, partial aggregation was noted. Comparisons between native and reduced gels indicated that aggregation was driven by disulfide bond formation occurring between LBP molecules. Two approaches are being pursued to alleviate this problem. a) We have mutated the two Cys residues in the LBP to Ala, and b) we are using the limited proteolysis experiments to identify a more cohesive domain for expression. We may also be able to get preliminary NMR spectra by rigorously maintaining a reducing environment. However, we know from gel shift data that the two Cys residues in the LBP are likely to be disulfide bonded in the native state, and reduction could cause an unwanted conformational change.

Assumptions

The only assumption being made for this task is that the bacterial monomeric protein will function like the high molecular weight form of the protein. The only published data indicate that, for binding to laminin-1, this is true [28]. Unsupported statements (no data given) in the literature question this finding [29]. Therefore, we will need to conduct a series of control binding experiments with the monomer. So far, our preliminary experiments indicate that the full length bacterial product interacts with laminin-1 in the same way as the high molecular weight mammalian protein does.

Results

As discussed in the "Methods" section, we have succeeded in generating efficient bacterial expression systems for both the full length LBP and the C135 ligand binding domain (Figure 1). The expressed proteins are readily purified over Ni columns using imidazole elution (Figure 2), and the poly-His sequence is efficiently removed using thrombin (Figure 3). After refolding the initially denatured bacterial expression product, the CD spectrum shows no evidence of random coil structure indicating that the protein has refolded well (Figure 4). The LBP CD spectrum is dominated by an alpha helical profile. Since the majority of the predicted alpha helix is in the C-terminal domain of the protein, we expect a largely alpha helical profile for the C135 LBP domain also. Figure 5 shows the mass spectra obtained for the isolated C135 LBP domain. **Both full length rLBP and C135 LBP were shown to bind to laminin-1 in ELISA assays (Figure 6). The pET--15b expression vector proved to be the best vector for this work. Partial aggregation of the recombinant C135 LBP domain at NMR concentrations was shown to be driven by disulfide bond formation and approaches have been taken to alleviate this problem.**

Discussion and Recommendations

The current bacterial expression system is working well, and could be used to provide heavy isotope labeled C135 LBP product for the NMR experiments. **Partial aggregation of proteins at high NMR concentrations is a well known problem, but we are fortunate in that the mechanism of LBP aggregation (i.e. disulfide driven) is amenable to corrective approaches.**

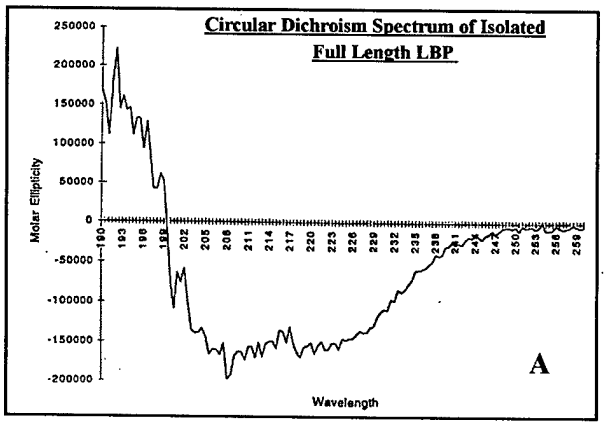

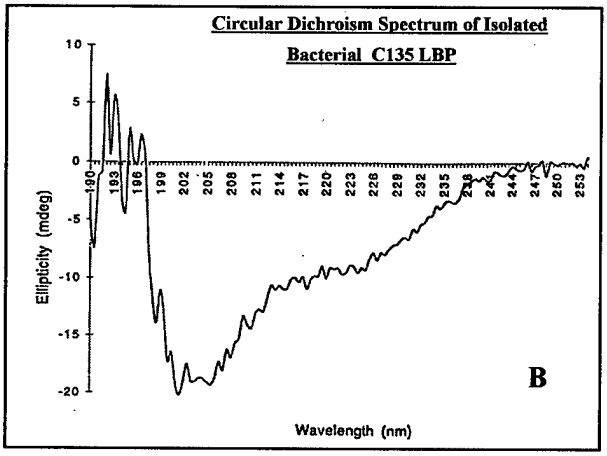

Figure 4. Circular Dichroism Spectra fpr (A) isolated mammalian 67 kDa LBP, and (C) recombinant C135 LBP matrix ligand binding domain.

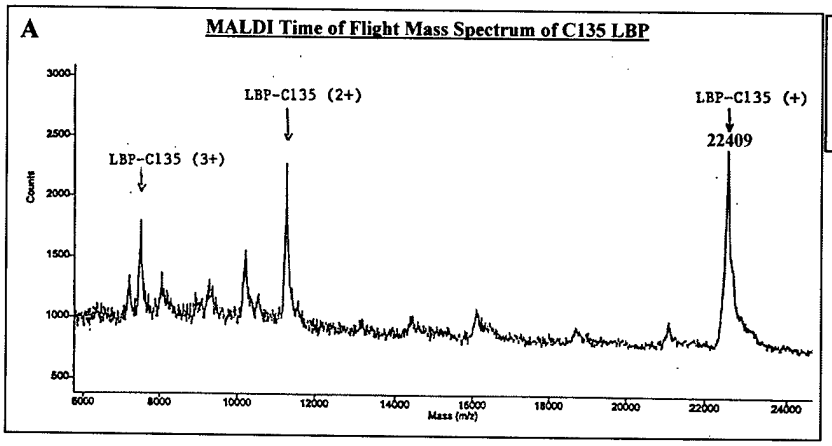

Figure 5. Mass Spectrometry analysis of the C135 LBP domain.

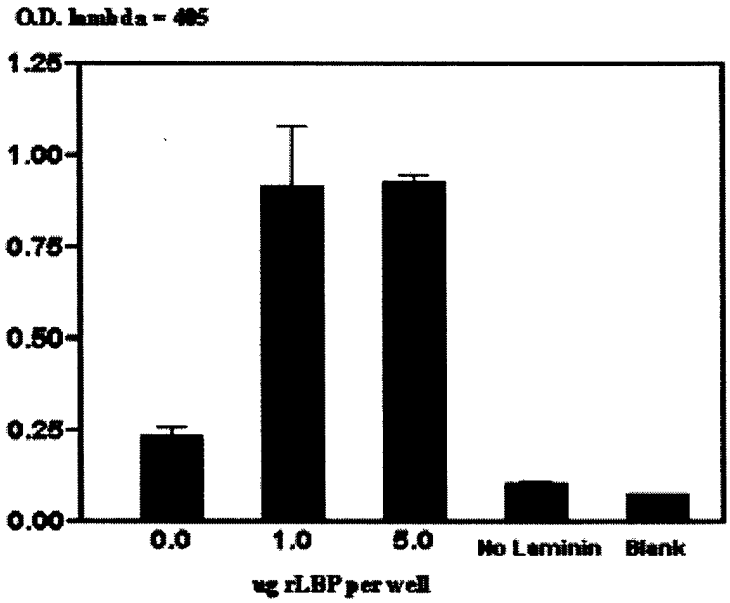

Figure 6. ELISA assay showing binding of laminin-1 to rLBP.

Progress on Technical Objective 1, task 3. (Bold = 2nd year activity)

Experimental Methods and Procedures

Although structural work on peptide 11 is exclusively supported by our NIH award, the data it provides is key to this Army project. Therefore, a brief update of the relevant recent findings is provided here.

Information about the orientation of required animo acid sidechains in the peptide 11 template is critical to the design of active peptido-mimetics. Unfortunately, there are very few NMR crosspeaks to the required Tyr, Ile or Arg sidechains in aqueous solution. We took advantage of the fact that the relatively viscous DMSO solvent would slow down the motion of the peptide and allow for better definition of individual structure conformations.

In this solvent we found a sufficient number of long range cross-peaks to allow for structure determination of the shorter peptide. The two-dimensional NMR spectra run in DMSO provided a greatly increased number of crosspeaks (by two to three fold) for all peptides studied, with several additional i,i+2 backbone NOEs over those seen in the aqueous spectra. The most NOEs were obtained when the peptides were first dissolved in water, were lyophilized and then redissolved in DMSO (called the hydrated state in this report). Under these conditions a residual water molecule appeared to stabilize the YIGSR region.

The spectra found in DMSO for the unhydrated and the hydrated states of YIGSR were very similar to each other. I,i+2 backbone NOE crosspeaks were found for C-terminal amide to serine, arginine to glycine and serine to isoleucine. The spectra for hydrated and unhydrated peptide 11 monomer in DMSO differed considerably from each other. The spectrum for the YIGSR region of hydrated peptide 11 monomer much more closely resembled those obtained for the YIGSR peptide itself. The spectrum of the YIGSR region in hydrated peptide 11 dimer also closely resembled the spectrum for YIGSR itself. The NMR spectra suggest that the water molecule stabilizes the YIGSR peptide by interacting with the tyrosine and the serine hydroxyl residues. This is also the case for the YIGSR domain in peptide 11 dimer. However, in the monomer the cysteine sidechain also appears to interact with the water, and this might destabilize the YIGSR domain. If this is true in aqueous solution, it could contribute to our observation of

better bioactivity for the dimer.

Assumptions

We assumed that the structure of the peptides in DMSO would be similar enough to the aqueous structures to provide useful data. Depending on the actual sequence of a peptide this may or may not be the case, and we do not yet know the situation for YIGSR/peptide 11.

Results

The new structural information about the orientation of the required amino acid sidechains in peptide 11 has been supplied to Dr. Wipke, and this has allowed him to make important adjustments to the input of the INVENTON program.

We do not yet have any detailed structural data on the ligand binding domain of the LBP which will enable Dr. Wipke to make additional adjustments to the INVENTON program pharmacophore. It should be noted that provision of structural data to Dr. Wipke is an ongoing process and happens throughout this project.

Discussion and Recommendations

The new information on required sidechain orientations in peptide 11, which we have already obtained, is important to drug design. **In the last year of this award, the anti-invasive/metastatic activity of candidate 16 will be evaluated, and Dr. Konopelski will synthesize several closely related mimetic compounds designed to clarify the optimal geometry for bioactivity. Data from these compounds will be used along with any structural information on the ligand binding domain of the LBP, to refine the INVENTON pharmacophore. INVENTON will then be used to generate second generation mimetics with better anti-invasive activity.**

Progress on Technical Objective 2, tasks 4 and 5. (Bold = 2nd year activities)

Experimental Methods and Procedures

Structural information from the full peptide 11 sequence is being derived because the minimal active domain, YIGSR, is too small to provide sufficient NMR crosspeaks. However, only the structure coordinates etc. for the YIGSR region are used in the drug design process. This provides a reasonably sized template for the design of non-peptide mimics. Design of potential mimics is carried out using the artificially intelligent program, INVENTON. The pharmacophore hypothesis provides the computer program with information as to what aspects of the peptide were likely important in recognition and binding with the LBP. The receptor (LBP) sees the shape of the peptide, and interacts with its electron density and dipolar nature. For template-based design, INVENTON uses the field of the template. Clearly, candidate structures must have chemically stable functionality. They must also survive the human digestive system to allow for oral therapy.

Now that we are working to obtain an NMR structure defining the ligand binding domain of the LBP, we will also be able to utilize characteristics of the LBP binding pocket in mimetic design. This was the original way INVENTON was used. The computer algorithms design specific mimics for the detailed bound structure completely automatically using FASM, fragment assembly for construction. After all structures are ranked, individual candidates are examined and molecular dynamics simulations are

performed to evaluate flexibility and the ability of the molecule to retain the desired conformation. Dr. Konopelski is responsible for evaluating the probable ease of synthesis of mimetics, and for choosing the actual synthetic approaches.

Assumptions

The main assumption in this part of the work is that the program INVENTON will design mimics which are at least as good as those designed by a human chemist. Our experience with the program working on other projects is that this is the case. Furthermore, the program is far more innovative, producing structures pharmaceutical chemists would not because of the biases in their training and professional experience.

Results

While Dr. Wipke's group have been working on refining the operation of the INVENTON program, no new runs have been made with the YIGSR structure. The next runs will be made after incorporating the new data on the orientations of the required amino acid sidechains and **with consideration of the bioactivity results from Dr. Konopelski's series of structural variants related to candidate 16.** This new structural input should provide a major refinement of the output "mimetics".

Discussion and Recommendations

We are close to testing the first synthetic mimetic designed by INVENTON **(candidate 16 - compound 1 in Progress on Technical Objective 2, Task 8)**. The results of this will tell us whether we are close to our goal of providing a sufficiently active lead compound, or whether major modifications will be needed. **The bioactivity results from the new structural variants of candidate 16 will guide us in the directions in which to make any modifications. Future additional runs with INVENTON will also incorporate structural information from the binding pocket of the LBP. INVENTON was originally designed to work with a negative template such as the binding pocket for peptide 11, and is most effective when doing this.**

Progress on Technical Objective 2, tasks 6 and 7. (All new material covering years 1 and 2; partial support from the State of California in year 1)

This work will be initiated with the new set of runs on INVENTON which incorporate additional information both from our structural templates (receptor bound peptide 11 and the LBP binding pocket), and from the bioactivity of Dr. Konopelski's new variant mimetics based on candidate 16. This represents a change in approach resulting from Dr. Konopelski's recent synthetic success in producing a suitable compound with many chiral centers.

Progress on Technical Objective 2, task 8.

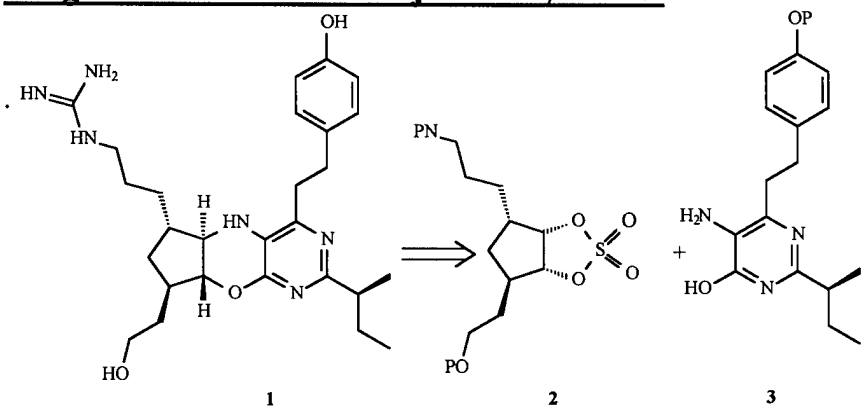

1 2 3

The work done by Félix Busquè Sànchez in the group of Professor Joseph P. Konopelski, has been focussed in the synthesis of one of the top candidate structures, the compound **1** (Scheme 1) also named candidate 16 by the INVENTON program.

Scheme 1. Target molecule and retrosynthetic analysis

This molecule is a structure with an excellent balance between synthetic accessibility and high ranking for biological evaluation. It is composed of a rigid core that presents the sidechains of the key aminoacids in the correct spacial orientation for maximum overlap with the defined conformation of peptide 11 bound to LBP.

Our first retrosynthetic analysis for this compound led us to the main fragments **2** and **3** (Scheme 1). The coupling of both molecules, removal of the several protecting groups and formation of the guanidine moiety should yield the desired compound **1**.

8.1.- Synthesis of fragment 2

The synthesis of an immediate precursor of the carbocycle **2**, with four chiral centers, has been completed in a diastereoselective fashion starting from the commercial alcohol **4** through the synthetic sequence outlined in Schemes 2 and 3. The synthesis starts with a nearly quantitative Swern oxidation of the alcohol **4** to give the ketone **5**, a Baeyer-Villiger oxidation of this compound, followed of a rearrangement in acid media provides the lactone **6**.

This unsaturated lactone **6** is regio- and stereoselective opened by the action of the corresponding organocopper reagent, yielding the unsaturated acid **7**. This S_N2'-*anti* selectivity is only achieved when a stoichiometric amount of CuBr-Me_2S is employed [30]. Reduction of the acid functionality with lithium aluminum hydride provides the alcohol **8**.

To continue the synthesis, we proposed a selective dihydroxylation of the terminal olefin present in the diene **8**. However, when this reaction was performed using the commercially available osmiun tetroxide dihydroxylation reagent AD-mix [31], the internal olefin was regioselective oxidized resulting in a mixture of the corresponding diastereoisomeric triols **9** in a 1:1 ratio. Unexpectely [32,33], no dihydroxylation of the terminal olefin was observed. Separation of the isomers can be effected by chromatography on column of silica gel and only one of them, **9a** (26% from **8**) believed to be the desired one, is carried on in the next series of steps.

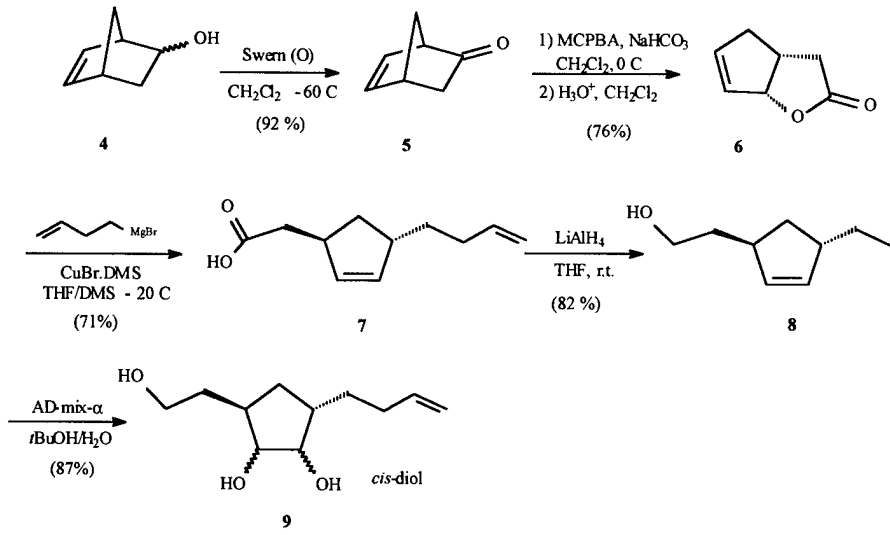

Scheme 2. Synthesis precursor of carbocycle **2**

The primary hydroxyl present in **9a** is selectively converted to the corresponding *tert*-butyldiphenylsilyl ether by a standard procedure (TPSCl, imidazole) [34] yielding the corresponding diol **10a**, which is protected as the Acetonide producing the compound **11a** (Scheme 3). The synthesis continues by elaboration of the side chain present in **11a**. This elaboration involves dihydroxylation of the double bond, oxidative cleavage of the resulting diol with sodium periodate [32] and reduction of the corresponding aldehyde **12a** with sodium borohydride to obtain the alcohol **13a**.

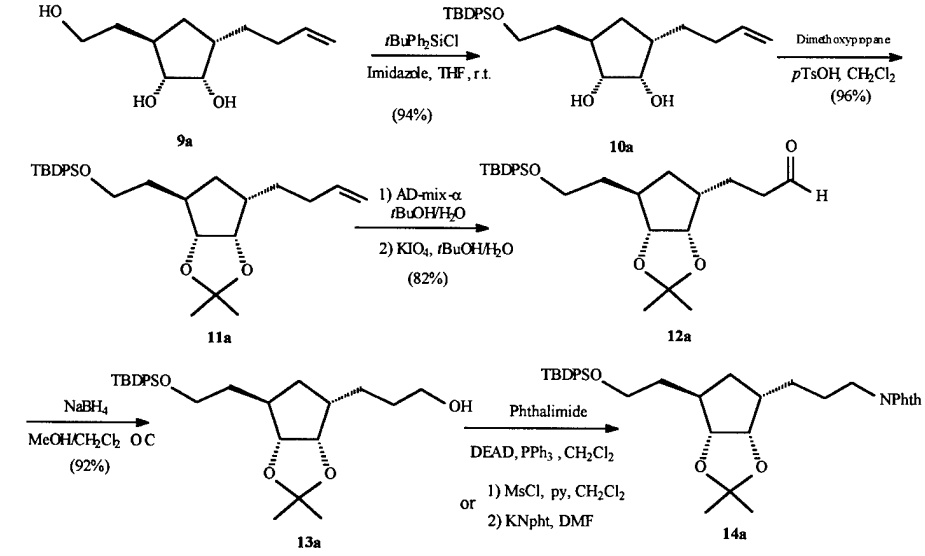

Scheme 3. Synthesis precursor of carbocycle **2**

The formation of the phthalimide derivative can be achieved in a single step by reaction of the alcohol **13a** with phthalimide using a Mitsunobu reaction [35], or in two steps by transforming first the hydroxyl in a good leaving group and performing then the nucleophilic substitution with potassium phthalimide [36]. In both cases, the compound **14a** is obtained in good yields (Scheme 3).

8.2.- Attempts to synthesize the fragment 3

The most interesting chemical feature of the pyrimidine **3** is the amine group present in the 5 position. For the synthesis of this heterocycle we envisioned 3 possible synthetic routes [37] depending of how the amine group could be introduced: primary synthesis, formation of a related 5-substituted pyrimidine which could generate **3** or elaboration of a simple pyrimidine with a masked amine in 5 position.

8.2.1.-Primary synthesis

The pyrimidine **3** could be formed directly by condensation between a β-ketoester, with a masked amine in 2 position, and the corresponding amidine (Scheme 4).

Several compounds with a nitrogen masked in the 2 position were tried as the β-ketoester component of the reaction. Unfortunately, at no point was there success in the formation of the pyrimidine ring, despite trying different reaction conditions of base, solvent and temperature (Scheme 4).

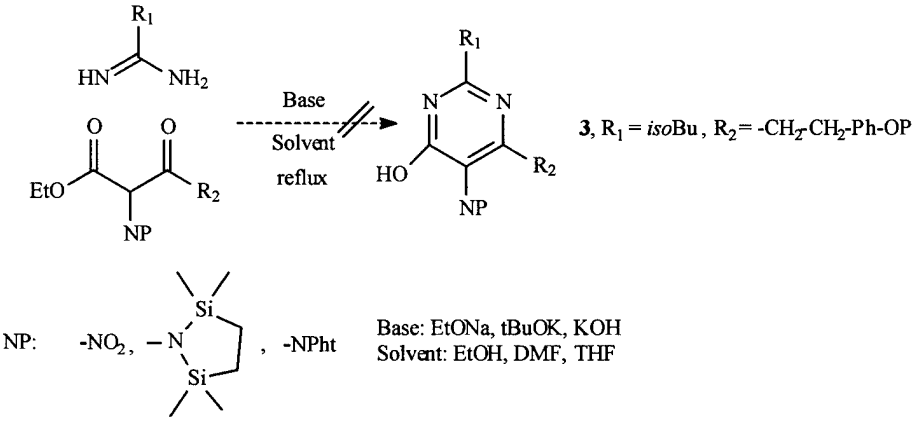

Scheme 4. Attempts of obtaining **3** by primary synthesis

8.2.2.- Synthesis from a related 5-substituted pyrimidine

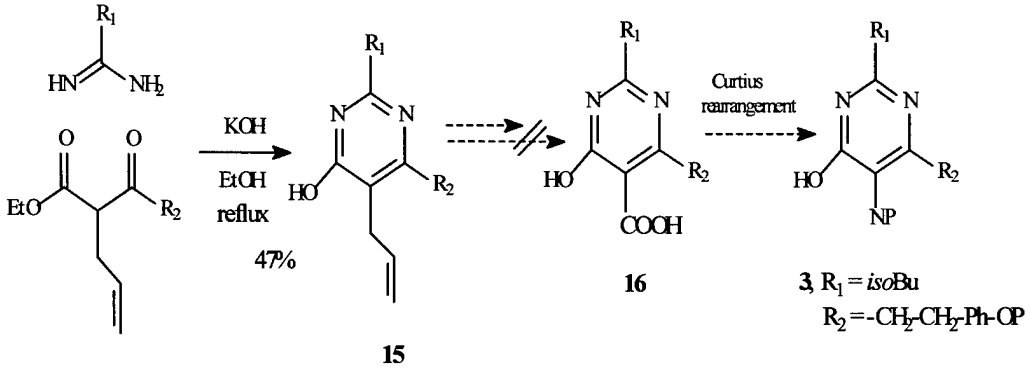

Scheme 5. Attempts of obtaining **3** by a modified Curtius rearrangement

The 5-aminopyrimidine **3** could be obtained from the carboxylic acid **16** by means of a modified Curtius rearrangement (Scheme 5) [38,38].

We attempted to synthesize the precursor **16** starting from the 5-allylpyrimidine **15**, but the poor yields obtained for the corresponding intermediates make us to abandon this synthetic route. Other 5-substituted pyrimidines more closely related to **16** than **15**, or **16** itself were not possible to obtain by primary synthesis from the corresponding precursors.

8.2.3.- Synthesis by elaboration of a simple pyrimidine with a masked amine in 5 position.

The pyrimidine **3** could also be obtained by adaptation of the literature procedure [39,40] outlined in Scheme 6.

Nitration of 4,6-dihydroxy-2-methyl-pyrimidine, **17**, followed by chlorination using phosphorus oxychoride affords the corresponding dichloronitropyrimidine **18**. This heterocycle reacts with diethyl malonate in light petroleum, in the presence of strong aqueous sodium hydroxide, to give the red salt **19**. Finally, decomposition of **19** in hot dilute hydrochloric acid yields the 2,6-dimethyl-4-hydroxy-5-nitropyrimidine **20**. In the original paper, reduction of the nitro group provides the corresponding aminopyrimidine **21**.

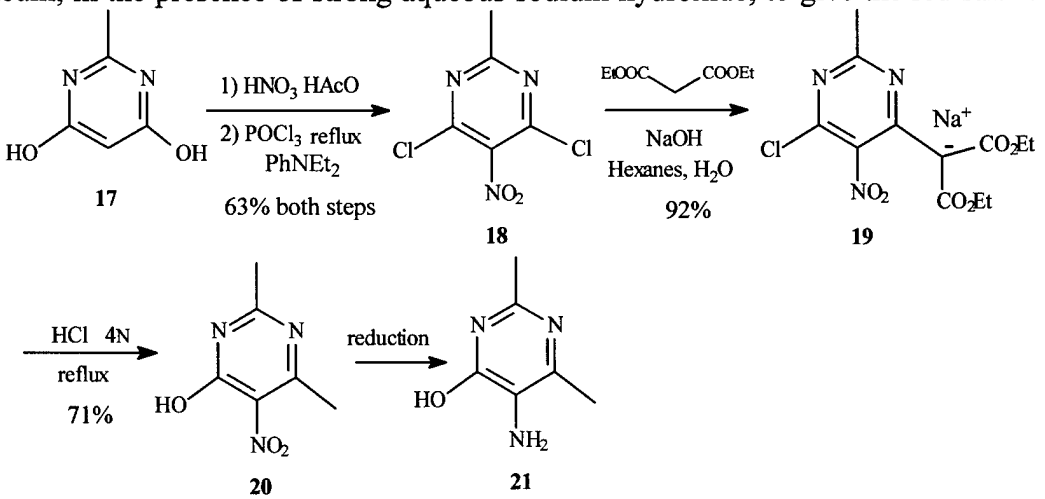

Scheme 6. Literature procedure for 5-amino pyrimidines

Using this procedure, a pyrimidine similar to **3** should be able to be obtained. The intermediate **22** (Scheme 7) was synthesized by benzylation of the salt **19** or directly from the dichloropyrimidine **18**; unfortunately, the next decarboxylation step did not work. The compound **20** can be chlorinated yielding the corresponding chloro-pyrimidine **23** (Scheme 7).

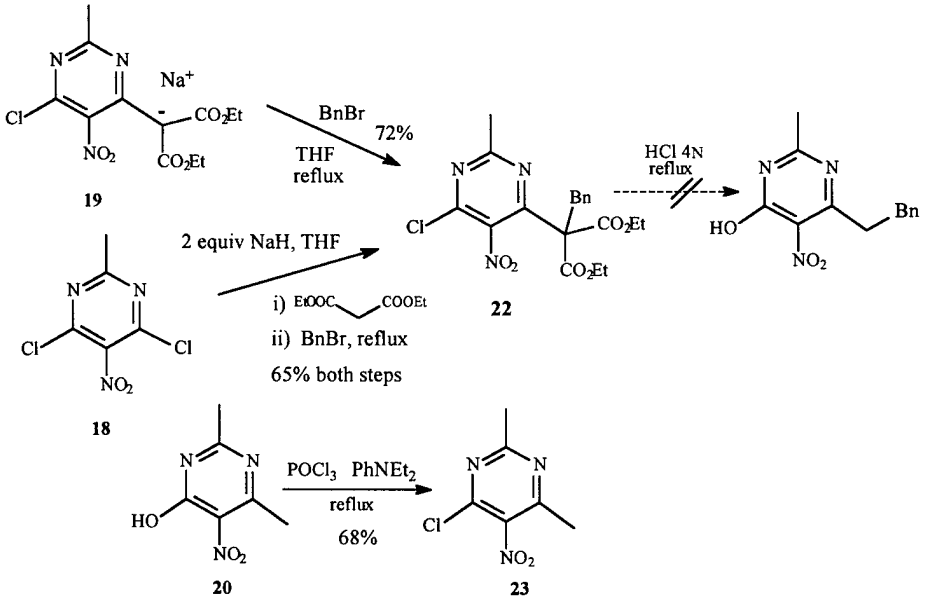

Scheme 7. Attempts of obtaining **3** from a simpler nitropyrimidine

8.3.- Attempts to follow the synthesis

Considering that the synthesis of the pyrimidine **3** had proven to be difficult to achieve, we decided to test the viability of the synthetic route using a model commercial pyrimidine.

Reaction of diol **10a** with diimidazolyl sulfate [41] produced the corresponding cyclic sulfate **24a**

(Scheme 8).

Reaction between the aminopyrimidine **25** and the electrophilic compound **24a** was expected to take place by S_N2 reaction of the free amine functionality with the cyclic sulfate. Attack must come from the same face as the pseudoserine side chain, and steric interactions should direct the attack to the desired position (Scheme 8). Surprisingly [42,43], the reaction did not work even at reflux of THF or CH_3CN, or at 60 °C in DMF.

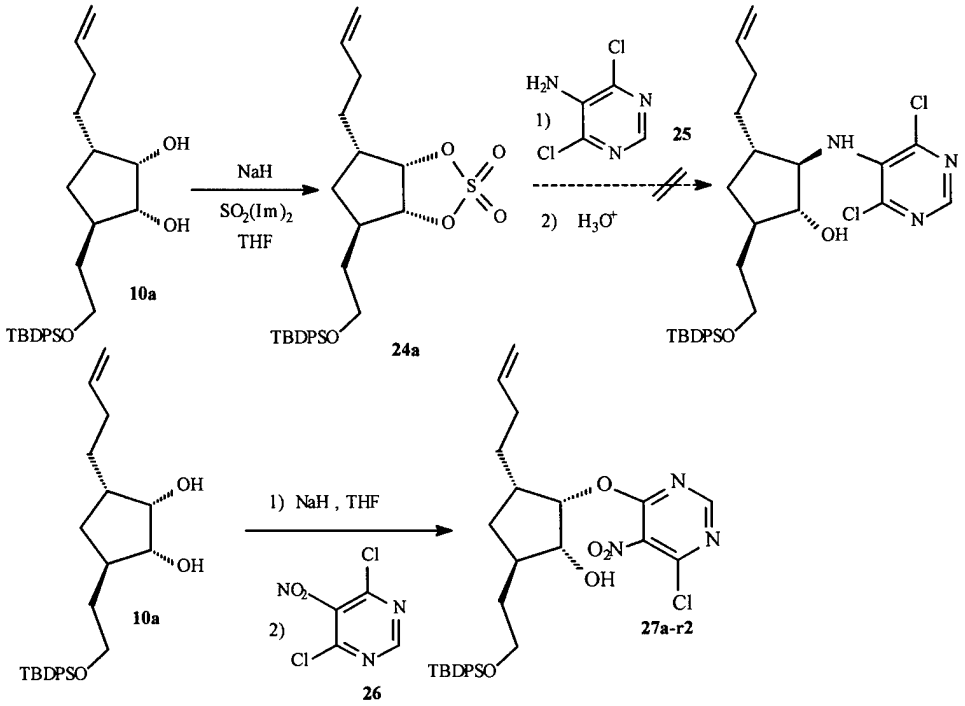

Alternately, the monoalkoxide of diol **10a** was found to react with the dichloronitropyrimidine **26** to give, with a low 17% of conversion, the unexpected diastereoisomer **27a** according steric considerations (Scheme 8). All the attempts to achieve this reaction by using conventional metal alkoxide combinations resulted in either similar low yields of desired product with recovery of starting material or in extensive decomposition.

Scheme 8. Testing the synthetic route with a commercial pyrimidine

Scheme 9. Coupling between diol **10a** and pyrimidine **26**

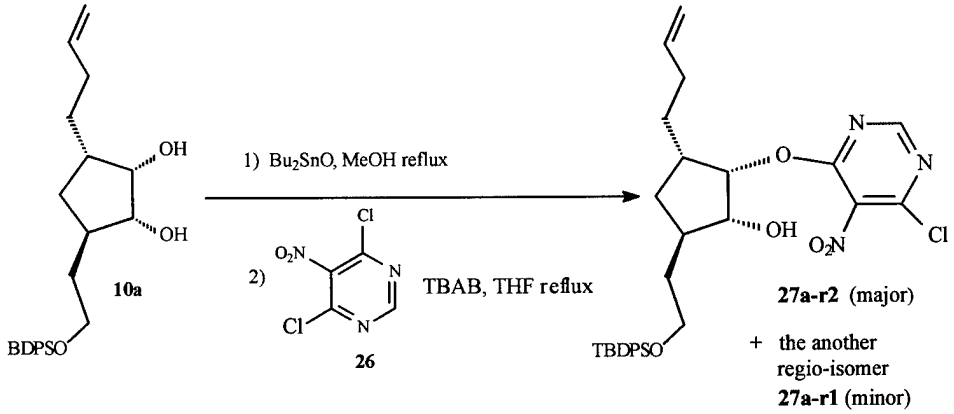

Finally, the coupling was achieved through the corresponding cyclic stannylene derivative (Scheme 9).

The reaction of diol **10a** with dibutyltin oxide in hot methanol gives raise to the corresponding tin ketal. This intermediate reacts with the pyrimidine **26** in the presence of TBAB in

THF to yield a 2:1 mixture of regio-coupled products **27a-r1** and **27a-r2** in a 65% yield (Scheme 9). *It has to be noted that this is the wrong regioisomer in order of achieving the synthesis of our target molecule.*

Considering all these results, we redesigned our synthetic route for the synthesis of the compound **1**.

8.4. New retrosynthetic analysis and progress towards the target molecule

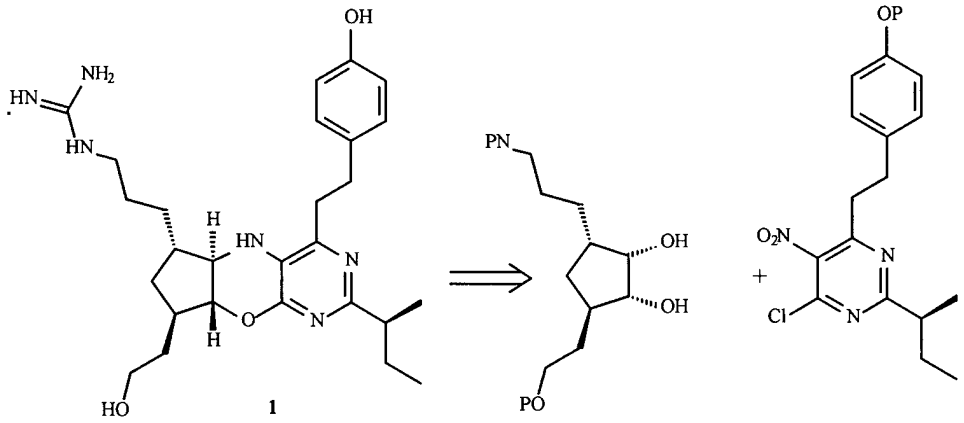

Our new retrosynthetic analysis for the target molecule **1** lead us to the main fragments **A** and **B** of the Scheme 10. Both fragments are intimately related with the previous **2** and **3**.

Scheme 10. New retrosynthetic analysis

In any case, the main goal of our synthetic work should be to find a synthetic method for obtaining the tricycle rigid core of **1**. After that, the protocols for the elaboration of the different side chains would be developed.

The first attempted alternative for obtaining the tricycle core of the target molecule was the outlined in the Scheme 11.

The coupling between diol **10a** and pyrimidine **22** was accomplished through the corresponding tin ketal intermediate, yielding a 1:2 mixture of regio-coupled products **28a-r1** and **28a-r2** in a 53% yield (Scheme 11). Remarkably, when this mixture was subjected to mesylation conditions with MsCl/pyridine it afforded only the mesylated regioisomer **29a-r2** with a 84% yield. *It has to be noted that this is the wrong regioisomer in order of achieving the synthesis of our target molecule.*

Reduction of the nitro group of this last compound with $SnCl_2$ [44,45] resulted in the formation of the tricycle amide **30a-r2** with variable yields from 60% to 10%. Unfortunately, when this amide was treated with NaH in THF the desired ring closing reaction for obtaining the tetracycle **31a-r2** did not happen. These reactions were performed on very small amounts of material and need to be repeated with our (new) best conditions.

Scheme 11. Synthetic alternative from diol **10a** and pyrimidine **22**

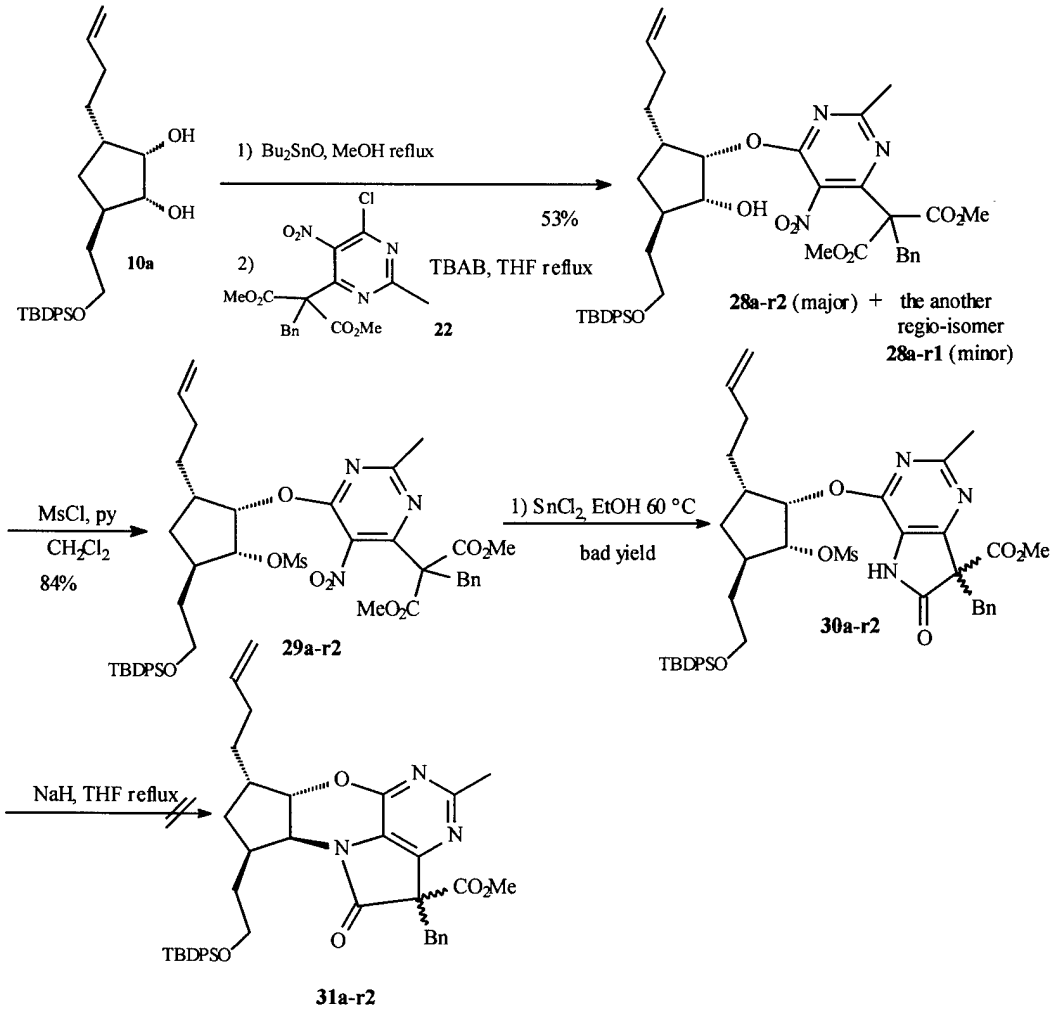

The second attempted alternative for obtaining the tricycle core of the target molecule was more successful and it appears in the Scheme 12.

The coupling between diol **10a** and the pyrimidine **23** was accomplished once more through the corresponding tin ketal intermediate, yielding a 1:3 mixture of regio-coupled products **32a-r1** and **32a-r2** in yields between 50% and 80% (Scheme 12). One of the factors affecting the yield of this reaction has proven to be the grade of conversion of starting diol. Again, when this mixture was subjected to mesylation conditions with MsCl/pyridine it afforded only the mesylated regioisomer **33a-r2** with a 87% yield. *It has to be noted that this is the wrong regioisomer in order of achieving the synthesis of our target molecule.*

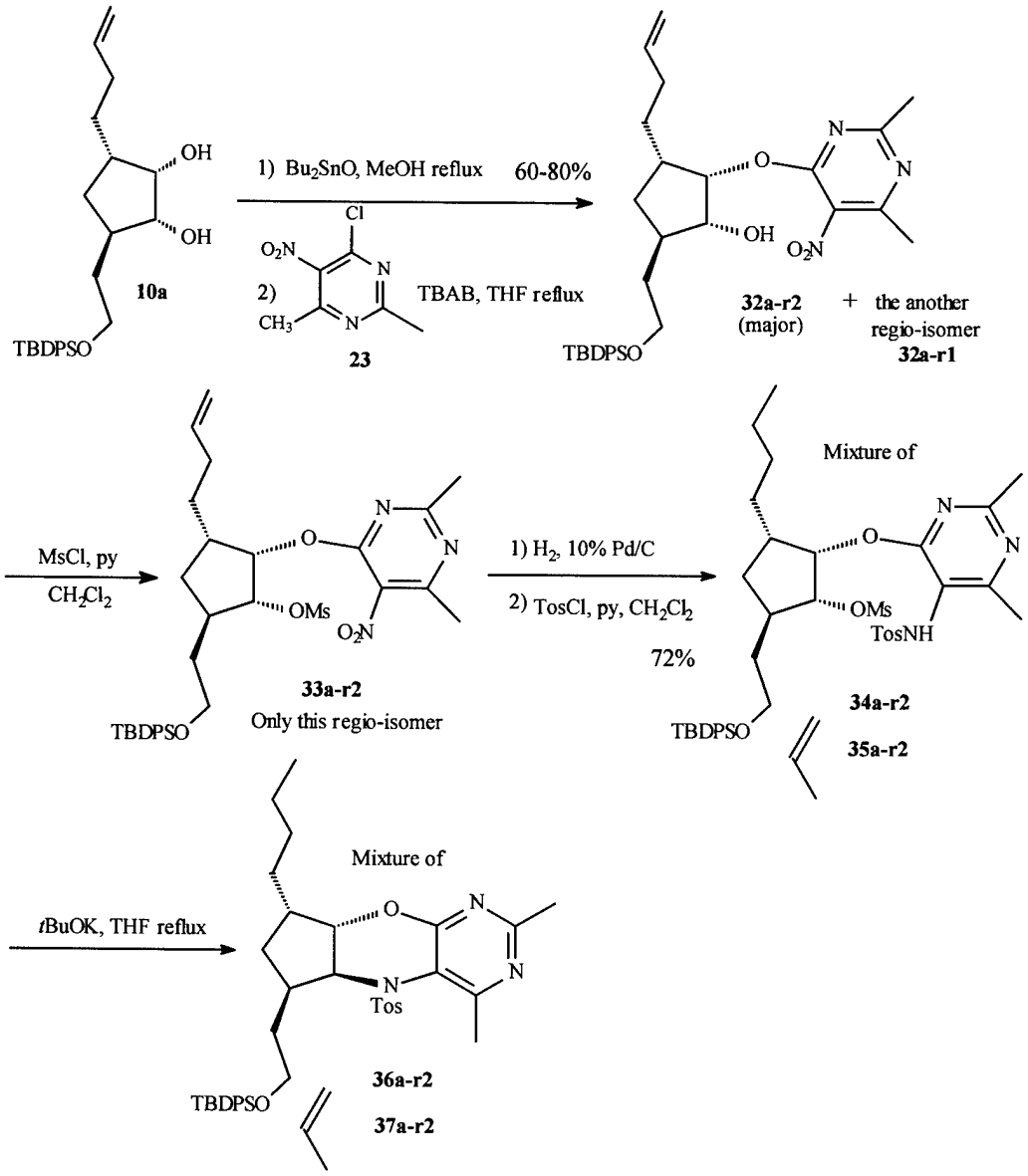

The reduction of the nitro group with $SnCl_2$ [44,45] resulted in the formation of the corresponding amine but in poor and irreproducible yields.

Alternately, the reduction was achieved by means of transfer hydrogenolysis using ammonium formate and 10% Pd/C [46]; the yields, if higher than in the case of using $SnCl_2$, were still variable. Moreover, the double bond of the side chain was always partially reduced.

Scheme 12. Successful approach to the synthesis of the tricycle

Finally, the best reducing method from the point of view of yield proved to be hydrogenation under pressure of hydrogen and 10% palladium on carbon (Scheme 12). Unfortunately, also in this case, the double bond was always partially reduced, obtaining a mixture of amines that were protected as the corresponding tosylated derivatives **34a-r2** and **35a-r2.** Expecting that the tosylate protection would make the amide proton acidic enough to be removed with different bases [47], the previous mixture was treated with NaH or with *t*-BuOK in THF. When using *t*BuOK as a base, the desired ring closing reaction was achieved, obtaining the mixture of tricycles **36a-r2** and **37a-r2** (Scheme 12). When using NaOH as a base, the closing reaction did not happen.

With the knowledge about how to close the middle ring, our next goal was to use in the ring closing reaction a more elaborated precursor (Scheme 13).

Scheme 13. Approach to the synthesis of the tricycle

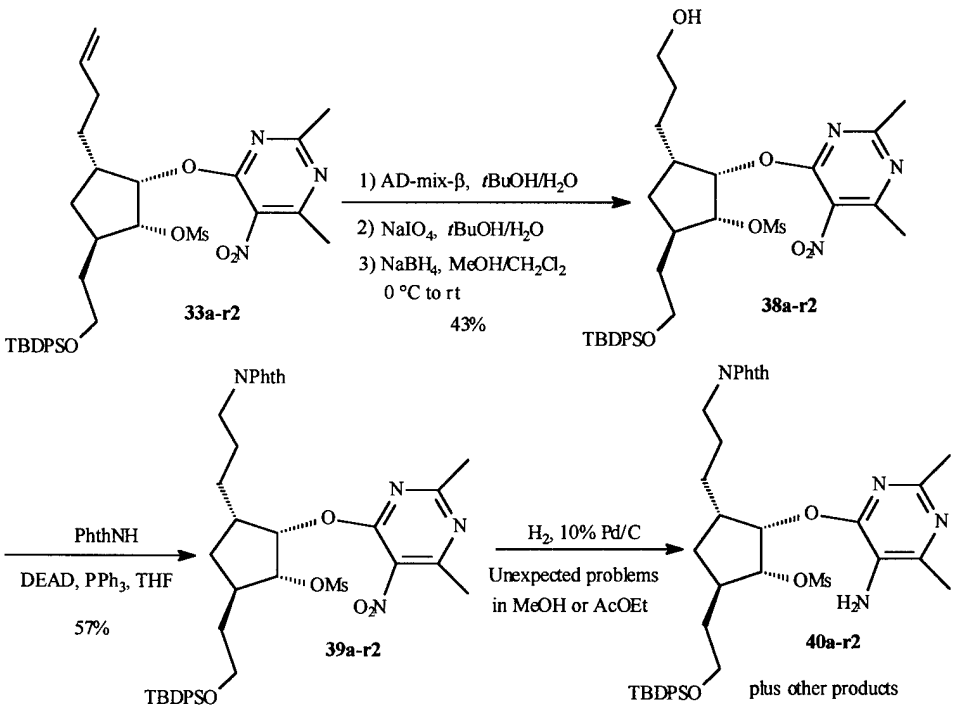

Dihydroxilation of the double bond present in the intermediate **33a-r2**, oxidative cleavage of the resulting diol with sodium periodate and reduction of the corresponding aldehyde with sodium borohydride afforded with a overall yield of 43% the alcohol **38a-r2** (Scheme 13). From this alcohol, the formation of the phthalimide moiety was achieved using a Mitsunobu reaction, affording with a 57% yield the desired compound **39a-r2**.

Until this point, the reduction of the nitro group using pressure of hydrogen with 10% Pd/C, the same protocol used with compound **33a-r2**, has proven to give problems yielding not only the expected amine **40a-r2** but also several impurities (Scheme 13).

Using our experience with this chemistry, we have recently succeeded in synthesizing a compound highly related to **candidate 16**. This synthesis begins with **4**, a commercial compound that is available in enantiomerically pure form. Thus, the reaction sequence can be used directly to obtain only one isomer.

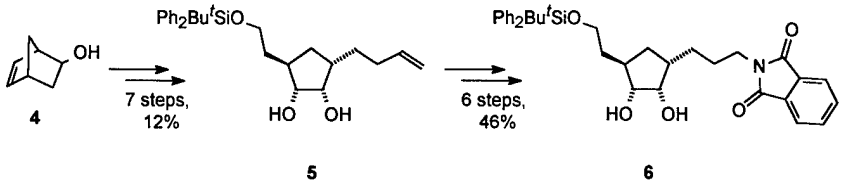

However, for the initial work it seemed reasonable to prepare the racemic mixture, with the idea of doing a resolution at the end and obtaining both enantiomers for testing. In this way, the initial synthetic venture produces two compounds for the Starkey group to test. Our current synthesis of **5** is executed from **4** in 7 steps and 12% overall yield. This compound is currently used in the coupling procedure to secure the tricyclic core of **candidate 16**. The transformation of **5** to **6** occurs in 46% yield over 6 steps. This sequence can be performed either initially (prior to tricycle formation) or at the end of the synthesis.

Results suggested that the isoleucine side chain in peptide 11 may act to reduce the conformational flexibility of the tyrosine aromatic ring, thereby positioning the phenol functionality in the proper space for binding. Given that **candidate 16** provides a rigid scaffold, the isoleucine side chain is not strictly required. Therefore, we prepared our first compound for testing from commercially available **7**. Nitration and chlorination afford fully substituted pyrimidine **8** in 51% overall yield. Treatment with malonate anion, followed directly with benzyl bromide, affords corresponding condensation product **9** in 65% yield from **8**. Future work will substitute a suitably protected 4-hydroxybenzyl bromide for benzyl bromide to incorporate the tyrosine side chain. Compound **9** reacts with the dibutyltin acetal of **5** to afford desired coupled material. Mesylate formation and reduction of the nitro group affords lactam **10** as a separable mixture of diastereomers rather than desired tricycle **11**. Treatment of **10** with base affords tetracyclic **12**, which has the desired scaffold in place *and holds the tyrosine side chain more rigidly than does* ***candidate 16***. Removal of the protective groups and elaboration of the guanidine functionality will afford one of the first compounds to be tested in the Starkey laboratory. As indicated earlier, the Konopelski group has been successful in synthesizing the rigid tricycle core. After that, the protocols for the elaboration of the different side chains were developed. With the exception of the tyrosine side chain, all the side chains have now been added to the tricycle core. Methods to elaborate the key tyrosine side chain have been tested with positive results, and will allow for the completed compound to be provided to Dr. Starkey this summer so that it can be tested for anti-invasive and anti-metastatic activity.

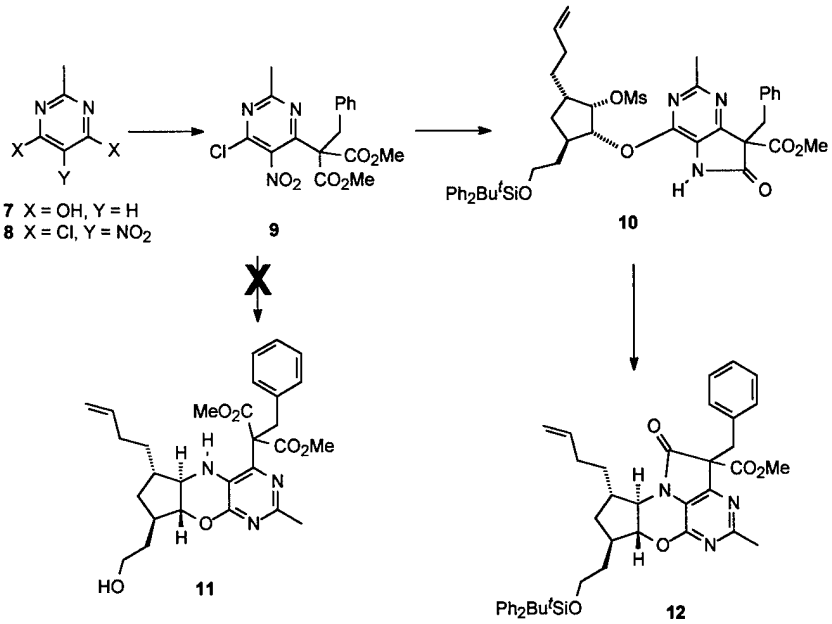

Assumptions

None

Results

A highly related compound to **candidate 16** is about to go into preclinical tests in the Starkey lab. This compound has been modeled and fits the original INVENTON pharmacophore as well as **candidate 16** does.

Discussion and Recommendations

With the installation of the tricyclic core in compound **12**, the route to a variety of materials based on the **candidate 16** structure is secure. Our plan is to generate a variety of closely related compounds in quick succession so as to produce of body of testing data. These data will then be evaluated to provide insights into structure-activity relationships and guide our future synthetic efforts to even more active compounds.

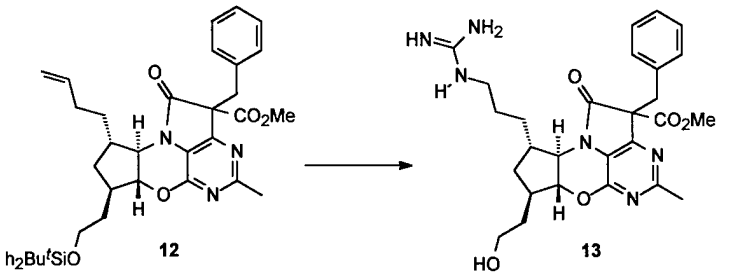

4 compounds - 2 diastereomeric pairs of enantiomers

4 separate compounds for testing by separation of diastereomers and enantiomers

Our plan calls for completion of the synthesis of **13** from **12**. This transformation will lead to four compounds, since **12** is actually a mixture of 2 diastereomers, each of which is a mixture of enantiomers. The diastereomers of **12** are easily separable by simple column chromatography, so each isomer is individually taken on to tetracycle **12**. To date we do not have structural information on the individual isomers, but we will perform a single crystal x-ray analysis on one compound to firmly establish the relative stereochemistry of all the chiral centers. In addition, we are beginning our resolution studies to determine the most efficient method for securing pure enantiomers. While the synthesis of **5** was developed to secure enantiomerically pure material, at this early stage of product formation and structure-activity relationships we choose to employ resolution methods to secure small quantities of enantiomerically pure material for testing rather than performing a total synthesis for each product.

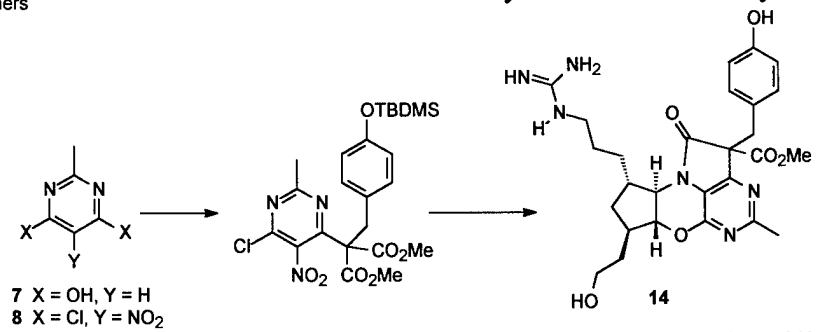

7 X = OH, Y = H
8 X = Cl, Y = NO_2

4 isomers comparable to those of **13**

A key compound will be **14**, in which the phenyl ring will be replaced by a phenol to afford a true tyrosine-type functionality. As mentioned earlier, this material will be synthesized by employing a protected 4-hydroxybenzyl bromide derivative in place of the benzyl bromide employed in the synthesis of **9**. At the present time we anticipate using a *tert*-butyldiphenylsilyl protective group, since this is the group we are currently using for the serine side chain. Both positions can then be deprotected in the same step. This should cause no major problems in the synthesis since this deprotection will be one of the last steps in the synthesis. This synthesis will again produce four compounds for testing, and these results will be directly comparable to those obtained from the isomers of **13**.

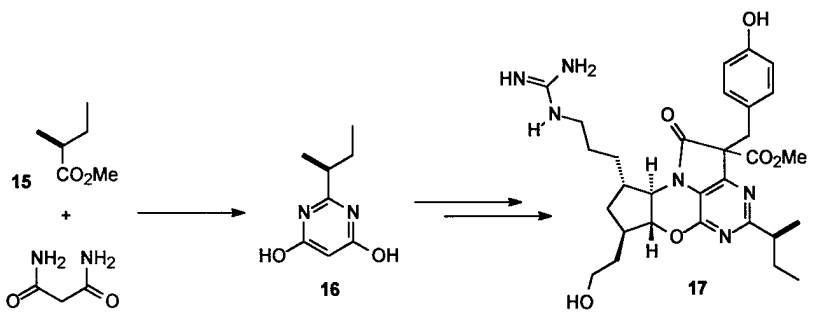

Introduction of the full isoleucine side chain requires the formation of a custom pyrimidine segment. Our proposed route involves condensation

of enantiomerically pure methyl 2-methybutanoate **15** [48] with malonamide to afford the corresponding pyrimidine **16**. The remaining chemistry toward **17** is identical to that already developed in our lab.

Compound **17** possesses the complete side chain array of **candidate 16**, but in addition has the lactam and ester functionalities originating from the malonate fragment in the synthesis of **9**. To date we have not attempted to remove these extraneous groups since the lactam brings two additional benefits to the design of **candidate 16**; namely, the extra rigidity in the tyrosine side chain and the presence of an additional chiral center. The ability to separate the diastereomers generated by this new chiral center will allow for a fine-tuning of the phenol position in a way that was not possible with the more mobile ethylene chain of **candidate 16**.

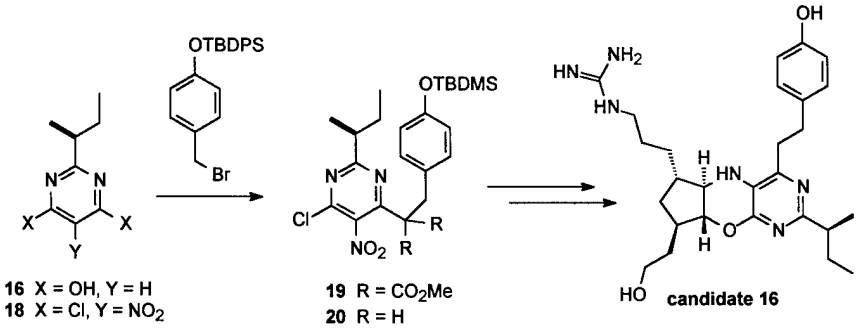

Nonetheless, we are still very interested in the formation of **candidate 16**. To this end, transformation of **16** to the corresponding 4,6-dichloro-5-nitro derivative **18** (required for production of **17**) and condensation with malonate anion and TBDPS-protected 4-hydroxybenzyl bromide will produce **19** in accord with the chemistry already developed. Decarboxylation methods will be employed at this point to secure desired **20**. Note that the hydrolysis of the malonate functionality will produce the pyrimidine 4-hydoxy derivative, which will have to be reconverted back to the 4-chloro material prior to reaction with **5**. The protocols already established in the laboratory for the production of **17** will afford **candidate 16** from **20**. Alternatively, we have recently performed the complete decarboxylation on **21**, the malonate addition

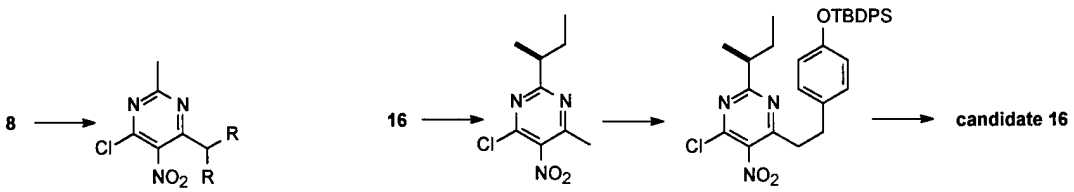

product of **8**. The three step procedure of malonate addition, hydrolysis, and chlorine reintroduction affords **22** in 60% overall yield. Substituting **16** into the reaction sequence for **8** would give a substrate (**23**) for deprotonation/alkylation [49] by TBDPS-protected 4-hydroxybenzyl bromide. Compound **24** leads directly to **candidate 16** by the established protocols.

Other derivatives of final materials **13**, **14**, **17**, and **candidate 16** are readily available and will be pursued if warranted by the testing results. For example, transformation of **5** to **6** involves an oxidative cleavage/reduction sequence (OsO_4 followed by $NaIO_4$, then $NaBH_4$) of the terminal alkene to afford alcohol, followed by introduction of the amine functionality. Direct hydroboration of the alkene would afford the corresponding alcohol with one additional carbon in the chain as compared to **5**, which leads to the corresponding homolog of **candidate 16**.

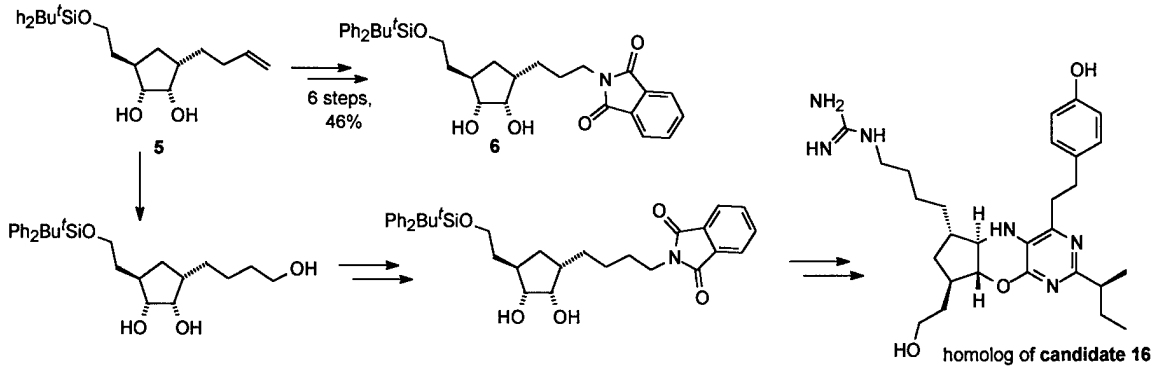

Progress on Technical Objective 3, task 9.

Experimental Methods and Procedures

Peptide analogs and mimetics of interest will first be tested for their general cytotoxicity in culture. This will be accomplished using the MDA-MB-231 human breast cancer cell line [50]. A maximal test dose of 1.0 mM (10 times the maximal dose of peptide 11 used to inhibit invasion in tissue culture) will be used. Other doses will be: 0.5 mM, 0.25 mM, 0.1mM and 0.05 mM. The MDA-MB-231 cells will be seeded at 4 x 10^5 per well in 12 well flat-bottomed tissue culture plates (six wells per data point). After overnight incubation in serum -containing medium, the medium will be replaced with serum -free medium or serum -free medium containing test compound. If problems are encountered with solubility, serum containing medium will be used during exposure to the test compound, and if problems persist, DMSO (1% or less) carrier will be utilized. Any compound that is still not sufficiently soluble, will be abandoned as unlikely to be able to be formulated for future preclinical/clinical testing. The cultures will be exposed to test compounds for 24 hours, then the medium will be removed, the cultures washed three times with serum free medium and refed with serum containing medium. After an overnight incubation, the cell number per well will be quantitated by incubating the cultures in MTT (3,[4,5-dimethylthiazol-2-yl]-2,5-diphenyltetrazolium bromide) (0.25 mg/ml) for three hours, removing the medium, dissolving the cells and purple MTT metabolite in DMSO, then measuring absorbance at $\lambda = 580$ [51].

Peptide analogs and mimetics that are not toxic in the above assay will be tested for their ability to inhibit invasion of breast cancer tumor cells through EHS basement membrane matrix (Matrigel) *in vitro*. Compounds will be tested against the estrogen receptor (ER) negative MDA-MB-435 [50] and MDA-MB-231 cell lines, as well as the ER+ve MCF-7 [50] and UISO-BCA-NMT-18 [52] human breast cancer cell lines. A "Transwell" system will be used to assay the ability of tumor cells to cross an 8 μ pore sized polycarbonate filter previously impregnated with a 1:20 dilution of Matrigel basement membrane matrix as described by Repesh [53]. This dilution provides for a relatively concentrated reconstituted matrix. As a consequence, the invasion rates are felt to be predominantly influenced by the ability of the cells to invade the matrix, rather than to be heavily biased by the physical ability of the cells to migrate through small pores [54]. The concentrated matrix slows down invasion, so that it takes from 3 to 5 days for enough cells to invade to the lower chamber for quantitation. Plates (24 well) containing Transwell inserts will be used.

Cells will be seeded at 5 x 10^4 cells per Transwell chamber in 0.2 ml complete medium, and 0.8 ml of medium will be added to the lower chamber. Fibronectin (15 μg per well as chemoattractant) will be added to the medium in the lower well in the case of MCF-7 cells which otherwise fail to invade in a reasonable time frame. Test compounds will be incorporated in the medium at 0.1 mM (molarity where peptide 11 gives 80% inhibition of invasion [18,55]), at 0.2 mM and 0.05 mM. Medium is changed daily in the Transwell experiments, and six Transwells are used per data point. A 0.1 mM peptide 11 data set will be included as a positive, and a 0.1 mM Acm-peptide 11 data set as a negative, control for LBP driven dimerization. The percentage of cells that have invaded through the Transwell membrane will be quantitated by measuring the purple MTT metabolite (see above). In this case, all cells in the upper chamber are removed with a Q-tip after MTT incubation and before dissolving the remaining cells in DMSO.

The lung colony assay is used to evaluate anti-metastatic activity. Tumor cells are harvested from subconfluent cultures with minimal trypsin/EDTA exposure. Prior to injection, mice are warmed at 37°C for 30 minutes. A set number of monodispersed tumor cells are injected per mouse in 0.2 ml via the lateral tail vein. Where the experiment requires co-injection of tumor cells with peptide, cells are prepared as indicated above. One mg peptide dissolved in the injection buffer is first loaded in 0.1 ml into the syringe, then the aliquot of tumor cells added in a further 0.1 ml. The contents of the syringe are gently mixed by inversion and injected as described above. The mice are killed several weeks later and autopsied. All tissues with suspect tumor colonies are rinsed in PBS and fixed in Bouin's fixative for gross and histological examination. The number of superficial nodules in the Bouin's-fixed tissues are determined using a dissecting microscope. We are now working exclusively with the highly invasive human breast cancer cell lines, MDA-MD-453 and MDA-MD-231. **For these lines, *SCID* mice are employed for the invasion assays. To facilitate the lung colony work, we have conducted serial selections in mice for high lung colonizing variants. This has been completed, and we have variants of both cell lines which reproducibly produce high lung colony numbers.**

Table 2. Selection of Efficient Lung colonizing Variants of the MDA-MB-435 Human Breast Cancer Cell Line

Selection	1st	2nd	3rd
Average number of lung colonies per mouse	12 ± 21	71 ± 99	152 ± 57

1 *SCID* mice injected with 5 X 10^5 tumor cells on day 1.

Assumptions

The general, and unavoidable, assumption made with the animal experiments is that human breast cancer cells will behave in *SCID* mice in the same way as they do in the human patient. There is also an assumption made that the "Transwell" in *vitro* invasion assay will reasonably predict anti-metastatic activity. After many years of experience with both assays, we are confident that the two assays give

roughly parallel results for the type of work being done on this project. Certainly, the *in vitro* assay is a useful screen before going into animal experiments.

Results

The NMR experiments, carried out under our NIH award, to determine the active conformation of peptide 11 utilized Tr-NOESY (Transferred Nuclear Overhauser Effect Spectroscopy) experiments where the peptide interacted with purified LBP. Dithiothreitol is used to prevent dimerization of free peptide 11, but was not used in the presence of the LBP which has an internal disulfide bond. Detailed examination of Tr-NOESY spectra revealed that the bound conformation of peptide 11 was dominated by a structure which could not be distinguished from synthetic peptide 11 disulfide dimer. Since peptide 11 can spontaneously dimerize under the conditions used in these NMR experiments, the presence of peptide 11 dimer was initially viewed simply as an unwanted complication.

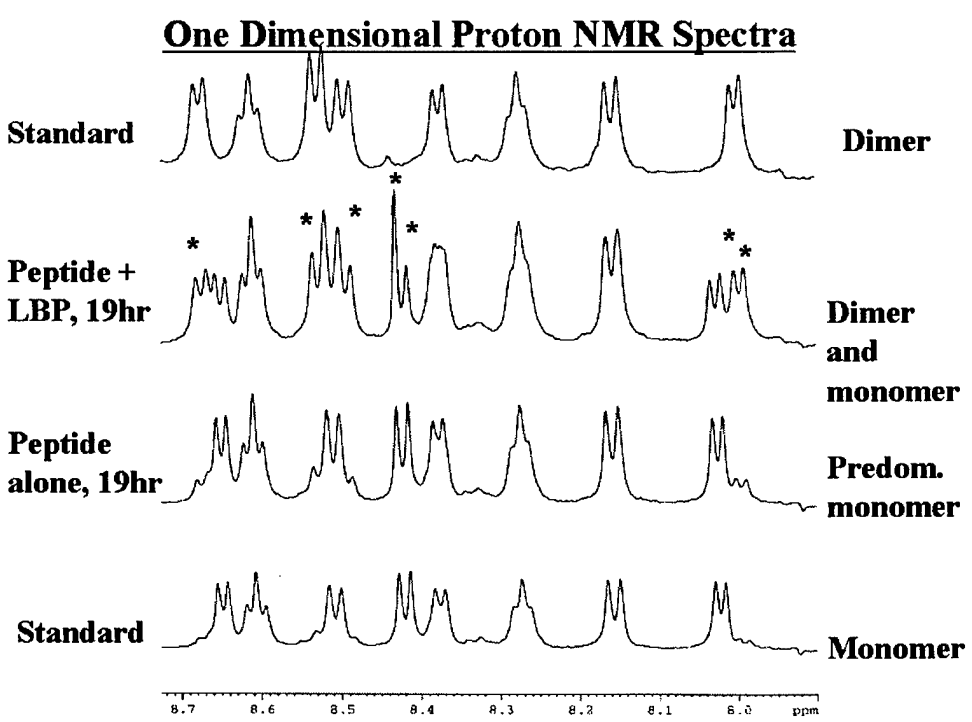

Figure 8. One dimensional proton NMR spectra of the fluoro-phenyl alanine containing peptide 11 analog over time in the presence or absence oof isolated LBP. After 40 hours in the presnce of the LBP the peptide reach a 100% dimeric state with a spectrum identical to the top one in this figure. A 32 fold excess of peptide over LBP was used in these experiments.

An analog of peptide 11 containing a para-fluoro substituted phenylalanine in place of the tyrosine residue was found to dimerize very much more slowly than peptide 11 in the absence of dithiothreitol (7-10 days compared with 6-7 hours for peptide 11 at room temperature at pH = 5.0). Surprisingly, this analog dimerized rapidly in the presence of the 67 kDa LBP (Figure 8). Rapid dimerization occurred when the peptide 11 analog was present in 32 fold excess of concentration over the LBP, and the rate of dimerization was found to increase with increasing concentration of the LBP. In this case, enzymatic activity of the 67 kDa LBP was suspected, and after appropriate controls were carried out, this was confirmed. **Similar results were obtained using N-acetyl peptide 11, which is somewhat less active than the non N-acetylated peptide and which also shows slow spontaneous dimerization. Both shed LBP and rLBP were able to facilitate refolding of denatured RNAase A (Figure 9).** Thus, the 67 kDa LBP appears to have a sulfhydryl oxidase or protein

disulfide isomerase activity. This activity was demonstrated for shed LBP isolated from conditioned tissue culture medium, for LBP isolated from EHS basement membrane matrix and for recombinant protein expressed in *E. Coli.*

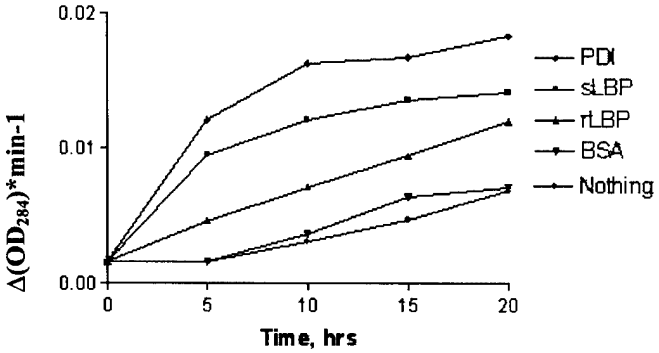

Figure 9. RNAase A refolding assay for sulfhydryl oxidase activity. RNAase activity assayed for 20 hours of refolding using 2':3'-cyclic cytidine monophosphate substrtate.

Because of its ability to produce disulfide bonded dimers, the Cys residue in peptide 11 was replaced with the conservative Ser substitution. We felt that this would simplify the structure determination of the bound peptide. Unexpectedly, this analog completely lost all bioactivity, a finding which suggests that dimerization is important to bioactivity. Given this preliminary data indicating that dimerization of peptide 11 might be involved in the bioactivities of the peptide, we compared the bioactivities of peptide 11, a non-oxidizable monomer of peptide 11 containing an Acm protected cysteine residue and peptide 11 dimer. The disulfide dimer was slightly more active *in vitro* (anti-invasion) and *in vivo* (anti-metastatic) compared to peptide 11, but significantly more active than the Acm protected peptide 11 monomer (Table 3., Table 4.). The Acm protected monomer was the least active in each case.

Table 3. - Effect of Monomeric and Dimeric Peptide 11 on CHODG44 Cell Invasion of Matrigel Basement Membrane Assayed using the In Vitro Transwell Assay

Peptide[1]	% Inhibition of Invasion
Peptide 11	51.2 ± 3.6
Acm-peptide 11	11.4 ± 10.1
Peptide 11 dimer	75.7 ± 4.1

[1]100μg peptide per ml medium.
[2]Each data point represents 6 replicates.

Table 4. - Effect of Monomeric and Dimeric Peptide 11 on Experimental Metastasis Formation by B16BL6 Cells

Peptide[1]	% Inhibition of metastasis	p value[2]
None	None	-
Peptide 11	45	0.017
Acm-peptide 11	20	0.154
Peptide 11 dimer	51	0.007

[1]1mg peptide used per mouse.
[2]Mann-Whitney U 2-tailed test. [3]n=7 mice.

We already knew, from our confocal microscopy studies [23], that the LBP is shed from invasive tumor cells in amounts proportional to their invasive properties. An experiment in which we propagated chinese hamster ovary cells in phenol red free medium, however, showed very little shedding. Since shedding from these cells was quite pronounced in phenol red containing medium,

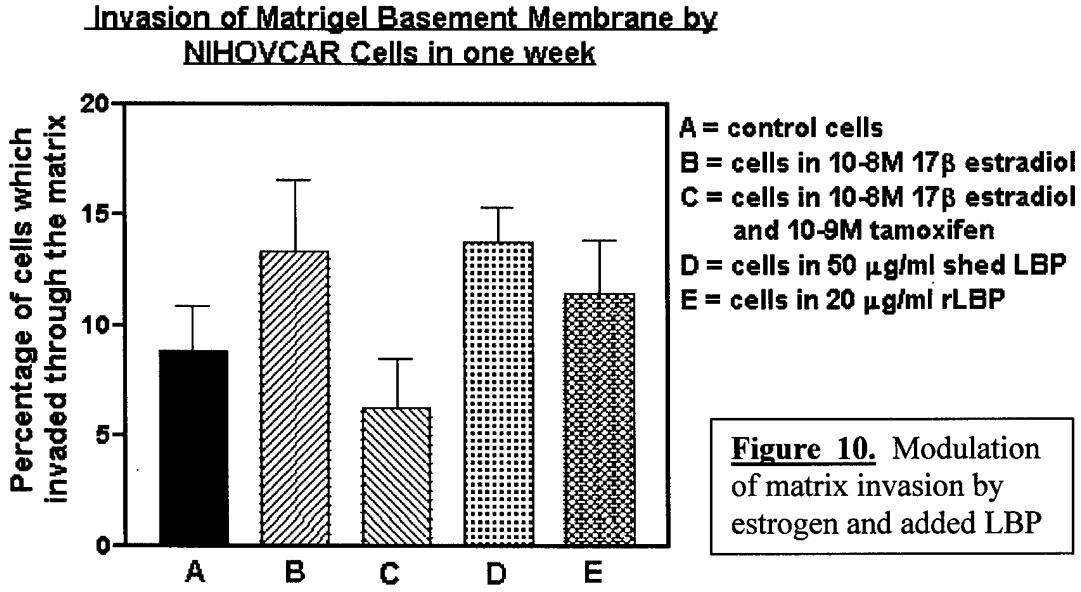

Figure 10. Modulation of matrix invasion by estrogen and added LBP

and since phenol red is an estrogen mimic, we hypothesized that shedding was responsive to estrogen levels. This was confirmed using the estrogen receptor (ER) positive human breast cancer, MCF-7 and ovarian cancer, NIHOVCAR:3 cell lines. Maximal shedding was noted at doses of 10^{-8} and 10^{-9} M 17β estradiol in phenol red -free, charcoal extracted, medium (Figure 11). The partial antiestrogen, tamoxifen, was able to block the shedding at doses 10 fold less than the level of 17β estradiol being used (Figure 10). We had already obtained evidence from our previous work with CHO cell variants that the level of shedding was proportional to the invasive potential [23], and we now found this to be true for these breast cancer and ovarian cancer cell lines also (Figure 10, Figure 11). These data support our hypothesis that shedding of the LBP might facilitate tumor invasion. The addition of µM concentrations of isolated LBP to the medium was found to promote invasion of the ER +ve cell lines in the "Transwell" assay (Figure 10). Thus, it appears that the mechanism of LBP shedding may be a legitimate therapeutic target.

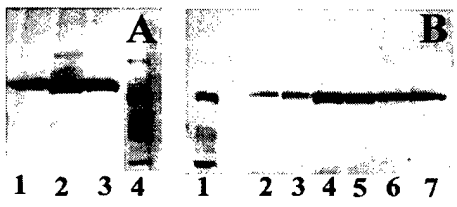

Figure 11. Silver stained SDS-PAGE gel of shed LBP affinity isolated from 3ml MCF-7 (A) and OVCAR (B) cell conditioned medium. Lanes 1,3 = 10^{-7}M, lanes 2,4 = 10^{-8}M and lanes 3,5 = 10^{-9} M estrogen.

Discussion and Recommendations

While any experimental data shedding light on the possible mechanisms of action of the 67 kDa LBP in facilitating tumor cell invasion and metastasis is very welcome, the apparent sulfhydryl oxidase/ protein disulfide isomerase enzymatic activity of the protein complicates the structural studies being carried out on the NIH award. Fortunately, the dimer is symmetrical, so all our previous work is valid. **Our NMR data suggest that the preliminary bound conformation we determined for peptide 11 is most likely bound peptide 11 dimer. The NMR experiments carried out in DMSO suggest similar structural attributes for YIGSR itself and the YIGSR domain in the peptide 11 dimer. It is important to note that YIGSR is just as active as peptide 11.** We expect to be able to elucidate why this short sequence is so active when we have determined the NMR structure of the LBP ligand binding domain. Most likely, the longer peptide requires interactions with the LBP at the N-terminal Cys residue as well as docking via the Tyr and Arg sidechains. The smaller YIGSR peptide may be able to fit into the binding pocket without the Cys interaction.

We are excited about the hypothesis that the mechanism of LBP shedding by invasive cells could represent a new therapeutic target, and a research grant proposal on this has been submitted to the DOD Breast Cancer Concept Award Program to explore this idea.

Progress on Technical Objective 3, task 10.

Work on this task will commence with the receipt of candidate 16 by the Starkey lab.

Key Research Accomplishments:

- **Successfully completed all preliminary experiments to determine the contact residues for peptide 11 in the LBP.**
- **Successfully identified regions in the LBP protein which interact with peptide 11 using phage display experiments.**
- **Successfully expressed the full length and the C-terminal ligand binding domain of the LBP in E. Coli.**
- **Successfully labelled rLBP with heavy isotopes for NMR spectroscopy.**
- **Determined the reason for aggregation of rLBP at high concentrations needed for NMR spectroscopy.**
- **Determined a successful synthetic approach for Candidate 16.**
- **Synthesized a very close structural relative to Candidate 16 which has the possibility for many small structural changes useful for determining the optimal geometry for bioactivity.**
- **Selected variants of the MDA-MB-435 and MDA-MB-231 human breast cancer cell lines which reproducibly produce good numbers of experimental lung colonies in *SCID* mice.**
- **Determined that cell shedding of the LBP facilitates invasion *in vitro*, and that it is sensitive to estrogen levels.**
- **Determined that the LBP has a sulfhydryl oxidase activity, and that dimerization of peptide 11 is important to invasion and metastasis.**

Reportable Outcomes:

1. Two manucripts have been published and a third comes out May 5 of this year.

   Kazmin,D.A., Hoyt,T.R., Taubner, L., Teintze,M., and Starkey,J.R. Phage Display Mapping for Peptide 11 -Sensitive Sequences Binding to Laminin-1 In Press, *J. Mol. Biol.* May, 2000.

   Starkey, J.R., Uthayakumar, S., Berglund, D.L. Cell surface and substrate distribution of the 67-kDa laminin binding protein determined by using a ligand photoaffinity probe. *Cytometry* 35:37-47, 1999.

   Starkey, J.R., Dai, S., Dratz, E.A. Sidechain and backbone requirements for anti-invasive activity of laminin peptide 11. *Biochim. Biophys. Acta* 1429:187-207, 1998.

2. One presentation was given at the 98 AACR annual meeting, and two invited seminars were given (Chemistry Department, University of California, Santa Cruz; NIH, NIAID Hamilton, MT).

3. Sublines of the MDA-MB-435 and MDA-MB-231 human breast cancer cell lines which are much more reproducible for lung colony assays were developed.

4. A new grant, based on work started under this award, has been obtained by Dr. Copié from the American Cancer Society Three other research grant applications are pending.

   Title = NMR Structure Determination of the Ligand-binding Domain of the 67 kDa Laminin Binding Protein
   Agency = ACS
   2 year award which activated Jan 1, 2000
   Total award = $380,000

5. Three predoctoral students, and one postdoctoral fellow, have worked on this project.

Conclusions

The major advances which were made in the first year of this award encompassed work aimed at elucidating the structure of the ligand binding domain of the 67 kDa LBP. Although difficulties with our isolation procedures for ligand derivatized LBP slowed down the studies on identifying the contact residues for peptide 11 in the ligand binding domain, the alternative approach of using phage display studies to pinpoint regions of interacting sequence worked very well. The phage display studies indicated that three separate sequence domains in the C-terminal domain of the LBP could interact with peptide 11. The phage display studies make a good start to mapping which LBP residues take part in peptide 11 binding. **This year, the success of our limited proteolysis experiments, has provided us with the protocols needed to undertake the work to define the contact residues for peptide 11 in the LBP. Therefore, this goal should be completed in the next six months.**

In order to undertake our NMR studies of the structure of the ligand binding domain of the LBP at reasonable cost, the binding domain needed to be expressed in a recombinant bacterial system. We accomplished this in the first year for the full length protein and for the ligand binding domain. In both cases, the *E. coli* strain expresses large amounts of poly-His tagged protein which is readily purified over a Ni affinity column. The poly-His tag is easily removed using thrombin cleavage, and the molecular weight of the expression products were confirmed by mass spectrometry. As judged by circular dichroism studies, the recombinant proteins refolded well. **This year, when we progressed to the preliminary experiments designed to guide us as to the best conditions to use to collect the relevant spectra, we found that the rLBP domain was partially aggregated at the high concentrations needed for NMR spectroscopy. Fortunately, the aggregation was shown to be disulfide driven, a situation for which there are remedies available. To avoid the aggregation, we have mutated the two Cys residues to Ala, and are currently expressing the modified rLBP. A second approach is to modify the protocols for preparation and spectroscopy so that everything is strictly anaerobic and reduced.**

The synthesis of candidate 16, which was designed by one of the early runs of the artificially intelligent INVENTON program, is essentially complete, and will be provided to the Starkey lab for bioactivity testing very shortly. The results of these tests are important, as they will indicate if the designed mimics are close to a potential drug lead, or if major modification to the INVENTON pharmacophore hypothesis will be needed. **Our plan, over the next year, is to synthesize a number of structural variants of candidate 16 and test these for bioactivity. These variants are designed to shed light on the optimal geometry for activity. The results of this testing will be incorporated into the INVENTON pharmacophore along with information from the structural studies of the LBP ligand binding domain. Second generation mimetics will be designed using the additional data, and are expected to be significantly more active than candidate 16.** This additional refinement will not happen until quite late in the project because the relevant data will not be available till then.

Finally, because some of our initial experiments indicated that the 67 kDa LBP could facilitate dimerization of peptide 11, we compared the anti-invasive and anti-metastatic activity of peptide 11, a

non oxidizable Acm protected analog of peptide 11 and peptide 11 dimer. The most active species was the dimer, with the Acm protected monomer being the least active in each case. **The total loss of activity which followed replacement of the Cys residue in peptide 11 with Ser, along with the previous results, suggests that dimerization is important to inhibition of invasion.** Interaction with the LBP via the N-terminal Cys residue is likely to be important to ligand binding of the longer peptide 11, while it appears not to be so for the short, very active, YIGSR peptide. Any structure which we derive for the "binding pocket" of the LBP will need to be compatible with these results. Along with possible requirements for sulfhydryl oxidase/disulfide isomerase activity, this consideration could provide some very useful constraints when we come to evaluate our future NMR derived structural data for the "binding pocket".

This project has taken longer than the originally planned two years. Two aspects of the project led to this situation. First, as can be appreciated from the appropriate section in this report, the synthesis of candidate 16 was much more challenging than we anticipated. It should be recognized that INVENTON does not design structures based on previous successful chemical approaches, rather it designs in an unbiased environment. Therefore, attempts to synthesize INVENTON structures often need to start from scratch. This was the case for candidate 16, and it took us a bit longer than we wanted to find the successful approach. The second aspect of the work, which required additional experimentation, was the number of unexpected new findings we uncovered with respect to the biology/biochemistry of the LBP. In order not to make avoidable mistakes later, we had to undertake a limited exploration of these new findings.

In the third year, with support from this award, we will evaluate the bioactivity of the candidate 16 mimetic and of the variants of this mimetic structure. This award will support all synthesis of the mimetics and the preclinical studies. We have been awarded a new grant (Dr. Copié as P.I.) from the American Cancer Society to continue the work on the structure of the peptide 11 binding domain of the LBP. This award was activated Jan. 1, 2000, and will allow us to continue this aspect of the project with uninterrupted support.

References

1. G. De Manzoni et al., *Oncology (Basel)* 55, 456-460 (1998).
2. M. I. Colnagi, *Adv.Exp.Med.Biol.* 353, 149-154 (1994).
3. K. Satoh et al., *Biochem.Biophys.Res.Commun.* 182, 746-752 (1992).
4. X. Sanjuán et al., *J.Pathol.* 179, 376-380 (1996).
5. M. G. Daidone, R. Silvestrini, E. Benini, W. F. Grigioni, A. D'Errico, *Br.J.Cancer* 76, 52-53 (1997).
6. G. Gasparini et al., *Int.J.Cancer* 60, 604-610 (1995).
7. D. Waltregny, L. De Leval, S. Ménard, J. De Leval, V. Castronovo, *Journal of the National Cancer Institute* 89, 1224-1227 (1997).
8. G. Pelosi et al., *J.Pathol.* 183, 62-69 (1997).
9. F. A. Van den Brule et al., *Eur.J.Cancer* 30A, 1096-1099 (1994).
10. P. Viacava et al., *J.Pathol.* 182, 36-44 (1997).
11. D. P. Pei, Y. Han, D. Narayan, D. Herz, T. S. Ravikumar, *J.Surg.Res.* 61, 120-126 (1996).
12. K. Mafune and T. S. Ravikumar, *J.Surg.Res.* 52, 340-346 (1992).
13. K. Narumi et al., *Jpn.J.Cancer Res.* 90, 425-431 (1999).
14. K. Satoh et al., *Br.J.Cancer* 80, 1115-1122 (1999).
15. J. Graf et al., *Cell* 48, 989-996 (1987).
16. Y. Iwamoto et al., *Science* 238, 1132-1134 (1987).
17. E. Ardini et al., *Mol.Biol.Evol.* 15, 1017-1025 (1998).
18. T. H. Landowski, U. Selvanayagam, J. R. Starkey, *Clin.Exp.Metastasis* 13, 357-372 (1995).
19. J. Yannariello-Brown, U. Wewer, L. Liotta, J. A. Madri, *J.Cell Biology* 106, 1773-1786 (1988).
20. V. Castronovo, G. Taraboletti, M. E. Sobel, *Cancer Res.* 51, 5672-5678 (1991).
21. K.-S. Wang, R. J. Kuhn, E. G. Strauss, S. Ou, J. H. Strauss, *J.Virol.* 66, 4992-5001 (1992).

22. Y. Kaneda et al., *Invasion Metastasis* 15, 156-162 (1995).

23. J. R. Starkey, S. Uthayakumar, D. L. Berglund, *Cytometry* 35, 37-47 (1999).

24. F. R. DeLeo et al., *Proc.Natl.Acad.Sci.U.S.A.* 92, 7110-7114 (1995).

25. G. Taraboletti, D. Belotti, R. Giavazzi, M. E. Sobel, V. Castronovo, *JNCI* 85, 235-240 (1993).

26. N. Guo, H. C. Krutzsch, T. Vogel, D. D. Roberts, *J.Biol.Chem.* 267, 17743-17747 (1992).

27. U. M. Wewer, G. Taraboletti, M. E. Sobel, R. Albrechtsen, L. A. Liotta, *Cancer Res.* 47, 5691-5698 (1987).

28. E. Y. Siyanova, *Bulletin of Experimental Biology and Medicine* 113, 70-72 (1992).

29. R. P. Mecham, *FASEB J.* 5, 2538-2546 (1991).

30. D. P. Curran, M. H. Chen, D. Leszczweski, R. L. Elliott, D. M. Rakiewicz, *J.Org.Chem.* 51, 1612-1613 (1986).

31. C. K. Hartmuth, M. S. VanNieuwenhze, K. B. Sharpless, *Chem.Rev.* 94, 2483-2547 (1994).

32. P. Wipf, Y. Kim, D. M. Goldstein, *J.Am.Chem.Soc.* 117, 11106-11112 (1995).

33. M. B. Andrus, S. D. Lepore, T. M. Turner, *J.Am.Chem.Soc.* 119, 12159-12169 (1997).

34. L. E. Overman and G. M. Rishton, *Org.Synth.* 71, 56-61 (1992).

35. O. Mitsunobu, *Synthesis* 1-28 (1981).

36. M. S. Gibson and R. W. Bradshaw, *Angew.Chem.Int.Ed.Engl.* 7, 919-930 (1968).

37. D. J. Brown, The chemistry of heterocyclic compounds; the pyrimidines (John Wiley and Sons, New York, ed. 52, 1994).

38. D. Kim and S. M. Weinreb, *J.Org.Chem.* 43, 125-131 (1978).

39. F. L. Rose, *J.Chem.Soc.* 4116-4126 (1954).

40. A. Albert, D. J. Brown, H. C. S. Wood, *J.Chem.Soc.* 3832-3839.

41. M. S. Berridge, M. P. Franceschini, E. Rosenfeld, T. J. Tewson, *J.Org.Chem.* 55, 1211-1217 (1990).

42. B. M. Kim and K. B. Sharpless, *Tetrahedron Lett.* 30, 655-658 (1989).

43. B. B. Lohray, Y. Gao, K. B. Sharpless, *Tetrahedron Lett.* 30, 2623-2626 (1989).

44. F. D. Bellamy and K. Ou, *Tetrahedron Lett.* 25, 839-842 (1984).

45. L. A. Agrofoglio, C. Demaison, L. Toupet, *Tetrahedron* 55, 8075-8082 (1999).

46. S. Ram and R. E. Ehrenkaufer, *Tetrahedron Lett.* 25, 3415-3418 (1984).

47. T. Tsunoda, J. Otsuka, Y. Yamamiya, S. Ito, *Chemistry Lett.* 539-542 (1994).

48. P. L. Anelli, F. Montanari, S. Quici, *Org.Synth. 69*, 212-219 (1990).

49. T. P. Murray, J. V. Hay, D. E. Portlock, J. F. Wolfe, *J.Org.Chem. 39*, 595-600 (1974).

50. X. Xie, N. Brunner, G. Jensen, J. Albrectsen, B. Gotthardsen, J. Rygaard, *J. Clinical and Experimental Metastasis 10*, 201-210 (1992).

51. A. M. Sieuwerts, J. G. Klijn, H. A. Peters, J. A. Foekens, *Eur.J.Clin.Chem.Clin.Biochem.* 33, 813-823 (1995).

52. R. R. Mehta, J. M. Graves, A. Shilkaitis, T. K. Das Gupta, *Br.J.Cancer* 77, 595-604 (1998).

53. L. A. Repesh, *Invasion and Metastasis* 9, 192-208 (1989).

54. A. M. Sieuwerts, J. G. Klijn, J. A. Foekens, *Clin.Exp.Metastasis* 15, 53-62 (1997).

55. G. J. Ostheimer, J. R. Starkey, C. G. Lambert, S. L. Helgerson, E. A. Dratz, *J.Biol.Chem.* 267, 25120-25128 (1992).